AD-A076 621 BERTRAM ASSOCIATES MERRIMACK NH F/G 8/3
REMOTE IDENTIFICATION OF A SALT WATER WEDGE THROUGH DISSIPATIVE--ETC(U)
OCT 79 C L BERTRAM , R A SHORE N00014-79-C-0160
UNCLASSIFIED NL

1 OF 2
AD A076621

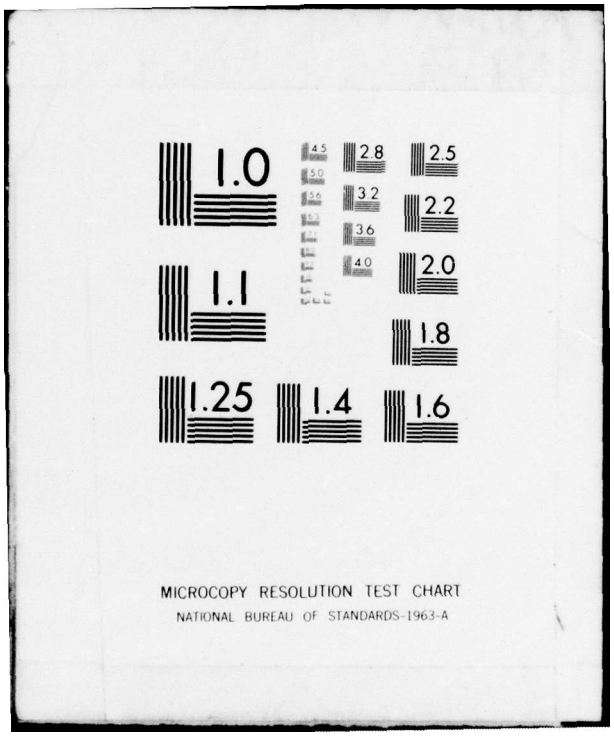
1.0
1.1
1.25
1.4
1.6
1.8
2.0
2.2
2.5
2.8
3.2
3.6
4.0
4.5
5.0
5.6
6.3
7.1
8.0
9.0
MICROCOPY RESOLUTION TEST CHART
NATIONAL BUREAU OF STANDARDS-1963-A

LEVEL II

12

REMOTE IDENTIFICATION OF A SALT WATER WEDGE THROUGH DISSIPATIVE MEDIA WITH A MONOCYCLE RADAR

Prepared By

C. L. Bertram
R. A. Shore

TECHNICAL REPORT NO. 1

October 1, 1979

This Research Was Supported By

The Office of Naval Research
Through Contract N00014-79-C-0160
Task Number NR387-105

BERTRAM ASSOCIATES
4 Maidstone Drive, Merrimack, NH 03054

ACKNOWLEDGEMENTS

The authors express there appreciation to Han Dolezalek and Commander Julian Minard of the Office of Naval Research for their encouragement and support. A special note of thanks is extended to William Whelan of Telecommunications Enterprises. Also particularly deserving the author's gratitude, without whose patience and technical typing this report would not have been as successful as it is, is Betty Bertram. Special thanks is given to Mr Joseph French for his computer programming effort.

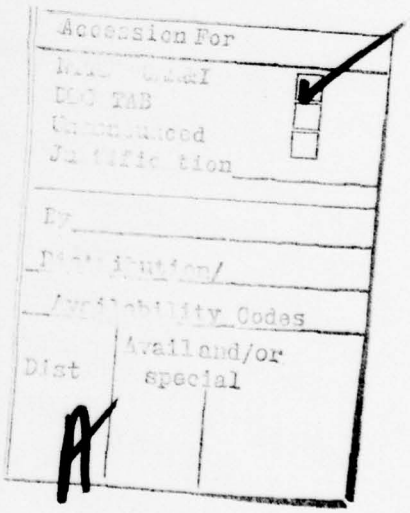

EXECUTIVE SUMMARY

One purpose of this study is to show theoretically the potential of a monocycle technique to detect and identify salt water wedges under dissipative fresh water. Also, the potential use for bathymetry is discussed, in particular for bodies of water of extremely low salinities as may be expected in some parts of the Baltic Sea, in Fjords and in large estuaries. The importance of bathymetry for military operations in shallow water is well known. It happens to be that some bodies of water with very low salinity are in areas of particular military sensitivity. Salt water wedges are of military importance for small submarines, swimmers and swimmer delivery vehicles and mine and counter mine warfare.

A monocycle pulse is either one half or one full cycle of a harmonic wave or square wave. It is the limiting of the harmonic wave or square wave in time that gives it its broadband characteristics. The broadband is not shifted up in frequency by a carrier because the monocycle is "carrierless". The duration of a monocycle can be microseconds, nanoseconds or picoseconds. Its harmonic analysis (Fourier transform from the time domain to the frequency domain) represents a broadband pulse that does not have a carrier.

The characteristics of a single cycle of short sinusoidal or square pulse of electromagnetic radiation are significantly different from the widely studied characteristics of single frequency pulse modulated continuous electromagnetic waves. Such a monocycle pulse undergoes a dispersion and

a change in amplitude when it is reflected from a boundary between media of different electrical conductivities, capacitivities (dielectric constants), and/or specific inductivities (permeabilities). The dispersion and amplitude change and consequently the resulting shape of the monocycle pulse depends on these differences in σ, ε and μ.

A computer model was developed to simulate a monocycle radar in air 15 meters over a layer of fresh water which is over a layer of salt water. The material that the layer consists of can be changed by changing the value of dielectric constant and conductivity, the constitutive parameters of the medium. The study using the computer model shows that it is possible to determine the difference between the transmitted monocycle pulse, the pulse reflected from the air/fresh water interface and the fresh water/ salt water interface by examining their shapes. The salt water layer was changed to simulate a sandy bottom and the pulse was compared to one reflected from the salt water layer. The pulses differed in both amplitude and shape implying it is possible to determine the difference between a salt water wedge and a sandy bottom by comparing the reflected pulses. The results are significant because they show that the method is applicable to detection and identification of salt water wedges beneath fresh surface waters. They also present a rapid remote method for use in bathymetry.

The analysis showed that, if it is assumed that the fresh water layer has a low conductivity of .02 mhos/meter, a monocycle radar 15 meters above the fresh water layer, transmitting a 10 ns pulse can detect a salt water wedge 13 meters below the fresh water. It is assumed that the trans-

mitted power is 10 decibels referenced to a Watt (dBW), the antenna, a folded dipole, has a gain of 0 dB, the minimum discernible signal is -120 dBW and the receiver bandwidth is 25% with a center frequency of 87.5 MHz. If a broadband folded dipole is used, an airborne antenna will have to be approximately 6 meters long to support the pulse. It may be possible to reduce the size of the antenna to 2 or 3 meters but probably at the expense of efficiency.

It it is assumed that the fresh water has a high conductivity of 1 mho/meter, the monocycle pulsewidth should probably be increased to 1 μs. The antenna is placed on the water to avoid the energy lost at the air/water interface and to take advantage of the loading of the water on the antenna. The high conductivity of the water will load the antenna by approximately a factor of 50 reducing its free space size from 610 meters to 12 meters. The concept of loading the antenna by a factor of 50 remains to be proven. Proof can be obtained by experimentation. If a broadband folded dipole is used, the antenna will have to be approximately 12 meters long to support the pulse. At the expense of efficiency, it may be possible to reduce the antenna to 6 or even 4 meters. The depth of which a salt water wedge can be detected using a monocycle radar with its antenna on water whose conductivity is 1 mho/meter is 5 meters. For this case, it was assumed that the transmitted power is 30 dBW, the antenna, a folded dipole, has a gain of 0 dB, the minimum discernible signal is -90 dBW and the receiver bandwidth is 25% with a center frequency of .875 MHz. If it is assumed that the antenna gain is -10 dB, the transmitter power will be increased to 40 dBW.

The computer model modified to simulate the temperature and salinities of the West Gotland Basin showed that, for a 100 ns pulse propagating through 5 meters of water with a conductivity of 1.2 mhos/meter, .28 mV/meter returned to the monocycle radar antenna on the surface of the water. The model also showed that when the conduction current dominates the displacement current delays in propagation as high as a factor of 80 can be expected.

For the final practical application a radar transmitter and receiver arrangement is visualized which emits a monocycle of an accurately determined waveform and investigates the waveform of each of the received return pulses which are backscattered from boundaries with varying σ,ε and/or μ.

ABSTRACT

This study investigates the characteristics of a single sinusoidal variation or single square pulse of electromagentic energy called a monocycle pulse. The study shows that the dispersion of the monocycle pulse is characterized by the boundaries from which it is reflected. The implication is that it is possible to detect and identify a salt water wedge under dissipative fresh water by examining the reflected monocycle.

A computer model was developed to simulate a monocycle in air or on a fresh water layer over salt water. The result of the model is that, if the fresh water has a low conductivity of .02 mhos/meter, a monocycle radar transmitting a 10 ns pulse 15 meters above the fresh water layer can detect a salt water wedge 13 meters below the air/water interface. If the conductivity is increased to 1 mho/meter and the radar antenna is placed on the water a salt water wedge 5 meters below the surface can be detected. The transmitted pulse was increased to 100 ns for this case. The computer results showed that the propagation of the monocycle pulse was slowed down by a factor of 80, depending on conductivity.

Results of particular military significance showed that a salt water wedge can be detected 5 meters below the surface of the air/water interface in the West Gotland Basin. The a 100 ns, 1 V/m incident pulse, .3 mV/meter returned to the antenna on the water. For the 10 ns pulse it is assumed that the receiver bandwidth is 75 to 100 MHz with a center frequency of 87.5 MHz. The 100 ns pulse is assumed to have a bandwidth of 7.5 to 10 MHz with a center frequency of 8.75 MHz. The results remain to be proven by experimentation.

ABBREVIATIONS AND SYMBOLS

c_1 = The velocity of electromagnetic energy in medium 1, meter/sec

c_2 = The velocity of electromagnetic energy in medium 2, meter/sec

d = The depth of the fresh water layer, meters

$e_r(t)$ = The field intensity of the reflected monocycle pulse as a function of time, Volts/meter

$|e_r(t)|_n$ = The normalized magnitude of the reflected electric field intensity, Volts/meter

$e_r(z,t)$ = The field intensity of the reflected monocycle pulse as a function of time and distance, Volts/meter

$e_t(t)$ = The incident or transmitted monocycle pulse for a uniform plane wave as a function of time, Volts/meter

$|e_t(t)|_n$ = The normalized magnitude of the incident electric field intensity, Volts/meter

E = The amplitude of a plane electromagnetic wave, Volts/meter

E_1 = The amplitude of E_{r1} at $z = 0$, Volts/meter

E_2 = The amplitude of E_{r2} at $z = 0$, Volts/meter

E'_2 = The amplitude of E_{r2} at $z = -d$, Volts/meter

E_3 = The amplitude of E_{t3} at $z = -d$, Volts/meter

E_{r1} = The amplitude of the electric field intensity after it is reflected from the air/fresh water interface, Volts/meter

E_{r2} = The amplitude of the electric field intensity in the fresh water after it is reflected from the fresh water/salt water interface, Volts/meter

$E_r(\omega)$ = The Fourier transform of $e_r(t)$

E_{t0} = The amplitude of E_{t1} at $z = 0$, Volts/meter

E_{t1} = The amplitude of electric field intensity in air, Volts/meter

E_{t2} = The amplitude of electric field intensity propagating in the fresh water, Volts/meter

E_{t3} = The amplitude of electric field intensity propagating in the salt water, Volts/meter

$E_{t0}(\omega)$ = The Fourier transform of E_{t0}

$E_t(\omega)$ = The Fourier transform of $e_t(t)$

E_{loss} = The integration loss

f = The frequency, Hertz

FET = Field Effect Transistor

FFT = Fast Fourier Transform

G = The antenna gain

H_{t0} = The amplitude of H_{t1} at $z = 0$, Amp/meter

H_{t1} = The incident magnetic field intensity in air, Amp/meter

j = $\sqrt{-1}$

k_m = The complex propagation constant of medium $m = \beta_m - j\alpha_m$, 1/meter

L = The height above the air/fresh water interface that the monocycle pulse is transmitted from, meters

MAAT = Maximum Allowable Attenuation

MDS = Minimum Discernible Signal, Watts

P_{ae} = Power reflected from air/dry earth interface, Watts

P_{ai} = Power reflected from air/glacial ice interface, Watts

P_{at} = Power reflected from air/trees interface, Watts

P_{aw} = Power reflected from air/water interface, Watts

$\overline{P}_r$ = The average echo signal from many independent scatterers, Watts

$P_r(\omega)$ = Power spectrum of $e_r(t)$

P_{sw} = Power reflected from the fresh water/salt water interface, Watts

P_t = Transmitted power, Watts

P_{th} = Power reflected from a thermocline, Watts

P_{wi} = Power in the fresh water layer, Watts

P_{air} = Power in air returned to the monocycle radar, Watts

R = Range, meters

R_1 = Height of radar above the fresh water interface, meters

R_2 = Range in the upper layer of the thermocline in fresh water, meters

R'_2 = Range in lower layer of the thermocline in fresh water, meters

$\overline{S}^2$ = The mean square slope of a rough surface

$\tan\delta$ = The loss tangent = the conduction current divided by the displacement current

T_1 = The Fresnel transmission coefficient at the air/fresh water interface

T_2 = The Fresnel transmission coefficient at the upper layer/lower layer of the thermocline interface

TE = Transverse electric wave, Volts/meter

TM = Transverse magnetic wave, Volts/meter

TEM = Transverse electromagnetic wave, Volts/meter

U = Wind velocity, knots

α_m = The attenuation constant of medium m, 1/meter

β_m = The phase constant of medium m, 1/meter

Γ = The Fresnel reflection coefficient for normal incidence at the air/fresh water interface

$\Gamma(\omega)$ = The overall Fresnel reflection coefficient where each spectral component is associated with a spectral component $E_r(\omega)$

$\Gamma_{m(m+1)}$ = The Fresnel reflection coefficient between layer m and layer m+1

Γ_{sw} = The Fresnel reflection coefficient at the fresh water/salt water interface

Γ_{th} = The Fresnel reflection coefficient of the thermocline

ε = The dielectric constant of any material, Farads/meter

ε_0 = The dielectric constant of free space (air), $\varepsilon_0 = \varepsilon_1$, Farads/meter

ε' = The dielectric constant of the material being investigated, Farads/meter

ε_{fw} = The relative dielectric constant of fresh water

ε_m = The relative dielectric constant of medium m

ε_r = The relative dielectric constant of any material, $\varepsilon_r = \varepsilon/\varepsilon_0$

ε_{sw} = The relative dielectric constant of salt water

ε_{w1} = The relative dielectric constant of the upper layer of the thermocline

ε_{w2} = The relative dielectric constant of the lower layer of the thermocline

$\bar{\eta}$ = The characteristic impedance of any material, Ohms

η_1 = The characteristic impedance of free space, Ohms

η_2 = The characteristic impedance of fresh water, Ohms

η_3 = The characteristic impedance of salt water, Ohms

η_m = The characteristic impedance of layer m, Ohms

θ_β = The 3 dB beamwidth of the antenna pattern in "azimuth", degrees

θ_i = The angle of incidence of the electromagnetic energy measured with respect to the normal to the mean plane of the randomly rough surface, degrees

λ_1 = The wavelength in free space, meters

λ_w = The wavelength in water, meters

μ = The magnetic permeability of any material, Henry/meter

μ_o = The magnetic permeability of free space, $\mu_o = \mu_1$, Henry/meter

μ_m = The magnetic permeability of medium m, Henry/meter

σ = The conductivity of any material, mhos/meter

σ' = The radar cross section of a target, $(\text{meter})^2$

σ° = Normalized Radar Cross Section (NRCS)

$\bar{\sigma}_i$ = The time average radar cross section of the i^{th} scatterer, $(\text{meter})^2$

σ_{fw} = The conductivity of fresh water, mhos/meter

σ_m = The conductivity of medium m, mhos/meter

σ_{sw} = The conductivity of salt water, mhos/meter

τ = The monocycle pulsewidth, seconds

ϕ = The depression angle (ϕ=0° on the horizon), degrees

ϕ_β = The 3 dB beamwidth of the antenna pattern in "elevation", degrees

ω = Angular frequency, radians/second

TABLE OF CONTENTS

LIST OF ILLUSTRATIONS

TABLES

SECTION I

INTRODUCTION

1.1 Background

The characteristics of a single cycle of a short sinusoidal or square pulse of electromagnetic radiation are significantly different from the widely studied characteristics of single frequency pulse modulated continuous electromagnetic waves. This is so because even if the pulses modulating the single frequency carrier are very short the receiver in typical radars filter out all of the frequencies except a few that exist around the carrier frequency. This filtering removes information that can be used to identify objects. Furthermore, if the modulating pulses are of the order of nanoseconds, the carrier frequency must be of the order of 10 - 100 GHz. Attenuation through dissipative media and even through the atmosphere is prohibitive at such high carrier frequencies.

A "monocycle" pulse is either one half or one full cycle of a harmonic wave or square wave. Theoretically it can be one half or one full cycle of any continuous wave. It is the limiting of the harmonic, square or in general continuous wave in time that gives it its broadband characteristics. The broadband is not shifted up in frequency by a carrier because the monocycle is "carrierless". The duration of a monocycle can be microseconds, nanoseconds and even picoseconds. Its harmonic analysis (Fourier transform from the time domain to the frequency domain) represents a broadband pulse that does not have a carrier.

Such a monocycle pulse undergoes a dispersion and change in amplitude

when it is reflected from a boundary between media of different electrical conductivities, capacitivities (dielectric constants), and/or specific inductivities (permeabilities). The dispersion and amplitude change and consequently the resulting shape of the monocycle pulse depends on these differences in σ, ε and μ.

This study investigates such dispersive effects.

1.2 Purpose

One purpose is to show theoretically the potential of the monocycle technique to detect and identify salt water layers (wedges) under dissipative fresh water. Also, the potential use for bathymetry is discussed, in particular for water bodies of extremely low salinities as may be expected in some parts of the Baltic Sea, in Fjords and in large estuaries. The importance of bathymetry for military operations in shallow water is well known. It happens to be that some bodies of water with very low salinity are in areas of particular military sensitivity.

Salt water wedges are of military importance for small submarines, swimmers and swimmer delivery vehicles and mine and counter mine warfare. To give a more detailed example, [1] members of the United States "Seal Team" penetrated 456 km (285 miles) up the Mississippi River by "riding" the fresh water/salt water wedge interface. The extremely rapid flow of the Mississippi makes this seem impossible. At the fresh water/salt water interface the flow is zero and minimum energy was expended by the "Seal Team".

The salt water wedge presents navigational problems. [2] If the propeller

of a ship is in the salt water wedge/fresh water interface, its energy is used to mix the two rather than propel the ship. The ship cannot maintain its course and if it turns sideways the Mississippi can capsize it.

Cook first presented the concept of using a monocycle radar in 1960. In his paper, "Proposed Monocycle-Pulse-Very-High-Frequency Radar for Airborne Ice and Snow Measurement" [3], he showed the feasiblity of using a monocycle radar to determine the thickness of ice and snow. It can be either one cycle or one half cycle of a harmonic wave. It is this limiting of the harmonic wave in time that makes it broadband.

1.3 Approach

For the final practical application an airborne radar transmitter and receiver arrangement is visualized which emits a monocycle of an accurately determined waveform and investigates the waveform of each of the received return pulses which are backscattered from boundaries with varying σ, ε and/or μ.

The approach is to initially work in the frequency domain. The single frequency results are then Fourier transformed into the time domain to give the optimum pulse shape for detecting salt water wedges in estuaries. The receiver bandwidth and sensitivity, repetition rate, transmitted power, Maximum Allowable Attenuation (MAAT), and antenna gain are determined from the optimum pulse shape and its spectral content.

An airborne monocycle radar over fresh water and salt water is computer

modelled. It is shown that it is possible to detect and identify a salt water wedge. The approach taken isolates the various areas where energy is lost so that they can be individually analyzed.

In Section 2, it is shown that surface roughness does not prevent the detection of salt water wedges. This is done by using Barrick's data for a rough surface.

Single frequency calculations are made in Section 3. Each harmonic wave is analyzed to determine how much energy is lost at the air/fresh water, thermocline and fresh water/salt water interfaces. The losses, including $1/R^2$ losses, are determined separately. The radar range equation is modified to include transmission through materials and focusing. Using the modified radar range equation, the maximum depth at which a salt water wedge can be detected is determined.

A computer model is developed in Section 4 that predicts the amplitude and shape of a pulse after it is reflected from a salt water wedge and sand. The analysis is performed for a narrow band pulse and a broadband pulse. It is concluded that to identify the material from which the pulse is reflected, it must be broadband. This excludes single frequency amplitude modulated radars. The model shows that it is feasible to detect and identify a salt water wedge using a monocycle radar.

In Section 5, a typical monocycle bathymetric radar is designed on a systems level. Various possible antenna configurations are discussed. A

transmit/receive network, FET preamplifier, bandpass filter, sample and hold circuit, integrator and microprocessor are discussed.

SECTION 2

SURFACE ROUGHNESS

2.1 A Rough Surface

It is the purpose of this section to show that if the frequency content of the pulse is kept below approximately 428 MHz the surface of the estuary seems smooth. This is done by interpreting Barrick's results for a rough [4] sea and applying them to monocycle illumination of an estuary. Since an antenna pattern has a finite beamwidth, the pulse will illuminate the surface over a range of angles. Three distinct regions of illumination are discussed. This is presented in case experimentation shows that the surface does not appear smooth. Except in certain instances where a one-way loss of 5 dB is assumed for a rough surface, the surface of the estuary in this report is taken as smooth.

Rough surfaces can reflect energy in unwanted directions reducing the effectiveness of the monocycle radar. A useful approximation is that the height of the waves is a random variable defined by a Gaussian distribution. From the random Gaussian distribution, the Normalized Radar Cross Section (NRCS) per unit area is found. [5] Presently accepted models of scattering surfaces are composed of larger gravity waves on which are superimposed smaller capillary waves. The problem of surface roughness referred to has been especially investigated for water surfaces in the open sea. Extrapolation of these results to bounded water surfaces such as an estuary seems reasonable as long as the estuarian boundaries are not too narrow.

Skolnik [6] depicts how the NRCS varies as a function of grazing angle and shows three distinct regions (see Figure 1):

1. An interference region
2. A plateau region
3. A quasi-specular region

The transition angle between the plateau region and the quasi-specular region occurs at a grazing angle of 60°.

Quasi-specular models are applicable to antenna radiation patterns with a beamwidth of ± 30°. For antenna radiation patterns with larger beamwidths, a combination of quasi-specular and diffused reflective models are used. The level of returned backscattered energy is considered to determine how much energy is reflected into the sidelobes and mainlobe of the antenna radiation pattern. Measured values of this return called the NRCS often lie between 0dB and 10 dB for medium seas at vertical incidence (see Figure 2). [7]

John Daley [8] presents an empirically derived model that agrees with both of two theories known as "Composite Surface Theory" and "Specular Point Theory" which are two of several theories trying to explain how electromagnetic waves are backscattered from a sea surface. The agreement is valid for vertical incidence. The frequencies used in his experiment are X band (8.91 GHz), C band (4.45 GHz), L band (1228 MHz) and P band (428 MHz).

Daley relates the NRCS to the average wind velocity by using a power law approximation:

$$\sigma^\circ = aU^x \qquad (1)$$

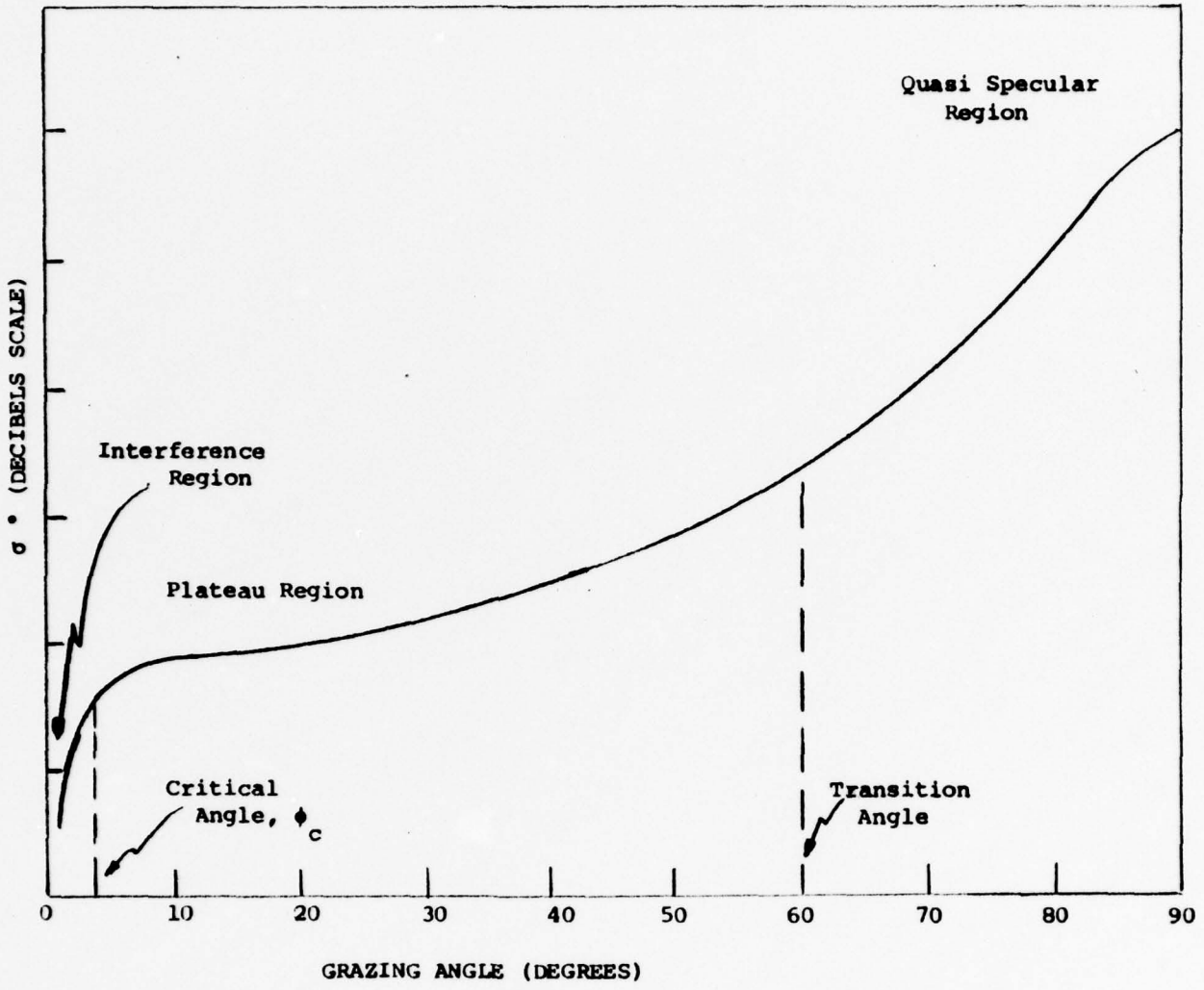

Figure 1. Representative example of the variation of σ° with grazing angle. [6]

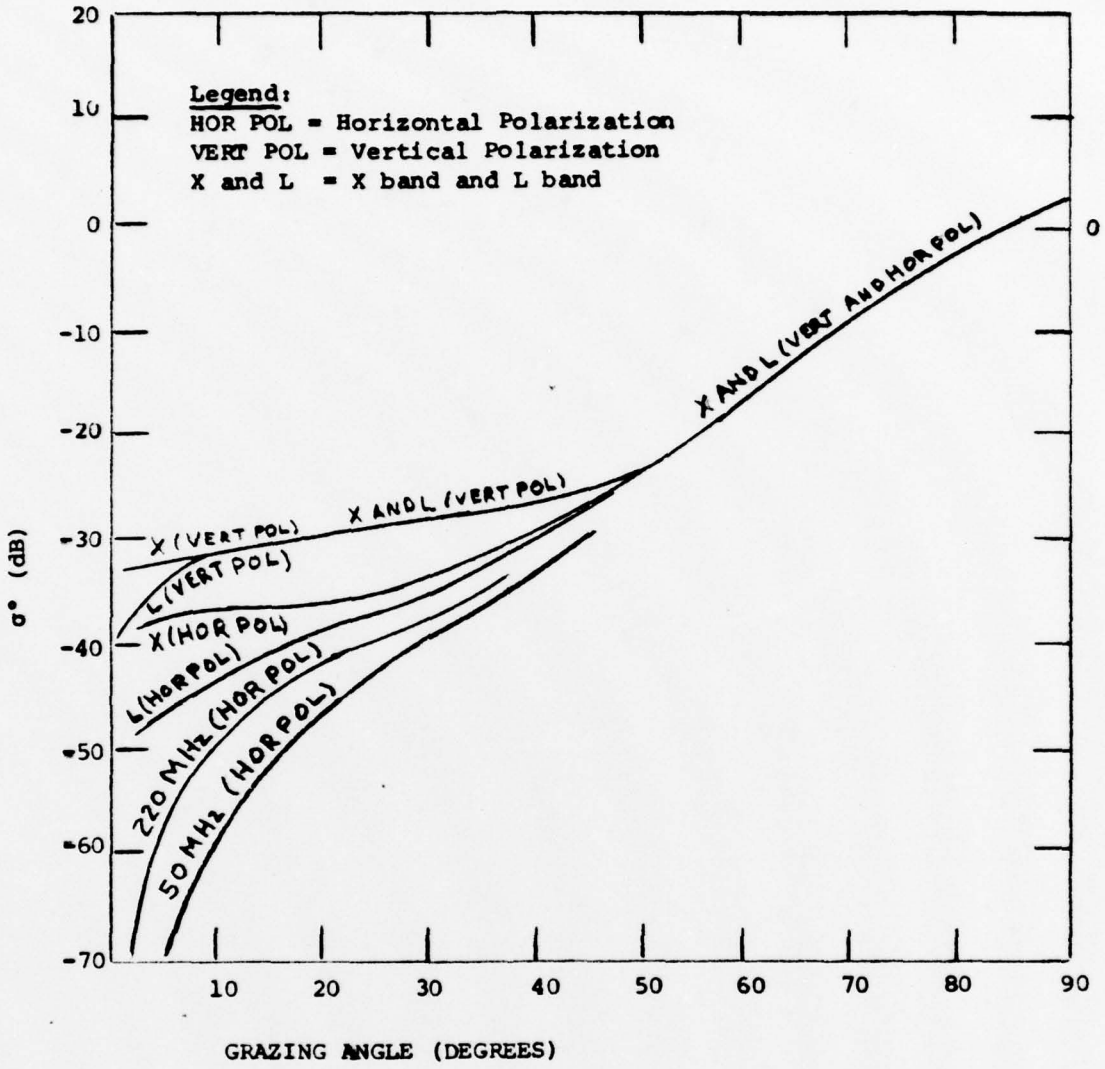

Figure 2. Composite of data showing the variation of σ° with grazing angle, frequency and polarization for a medium sea. [7]

where

$$\sigma^\circ = \sigma'/A = \text{NRCS} \qquad (2)$$

and

σ' is the radar cross section of the target [9] in square meters

A is the area on the surface illuminated by the two-way antenna pattern [10]

U is the wind velocity

He determines a and x from a least squares fit to test data.

Barrick [11] shows that the NRCS for a rough surface with a Gaussian distribution is

$$\sigma^\circ = \frac{\sec^4\theta i}{\overline{s}^2} \exp\left(-\tan^2\theta i/\overline{s}^2\right) |\Gamma|^2 \qquad (3)$$

where

Γ = The Fresnel reflection coefficient of the air to surface interface for normal incidence

$\overline{s}^2$ = The mean slope of the rough surface

θ_i = The angle of incidence of the illuminating uniform plane wave measured with respect to the normal to the mean plane of the random surface

Daley et al [12] show the median decibel values of NRCS for wind velocities of 0-50 knots at vertical incidence for X, C, L, & P band (see Figure 3). At P band the median NRCS is approximately 2 dB. This value is equal to the Fresnel power reflection coefficient for a smooth sea.

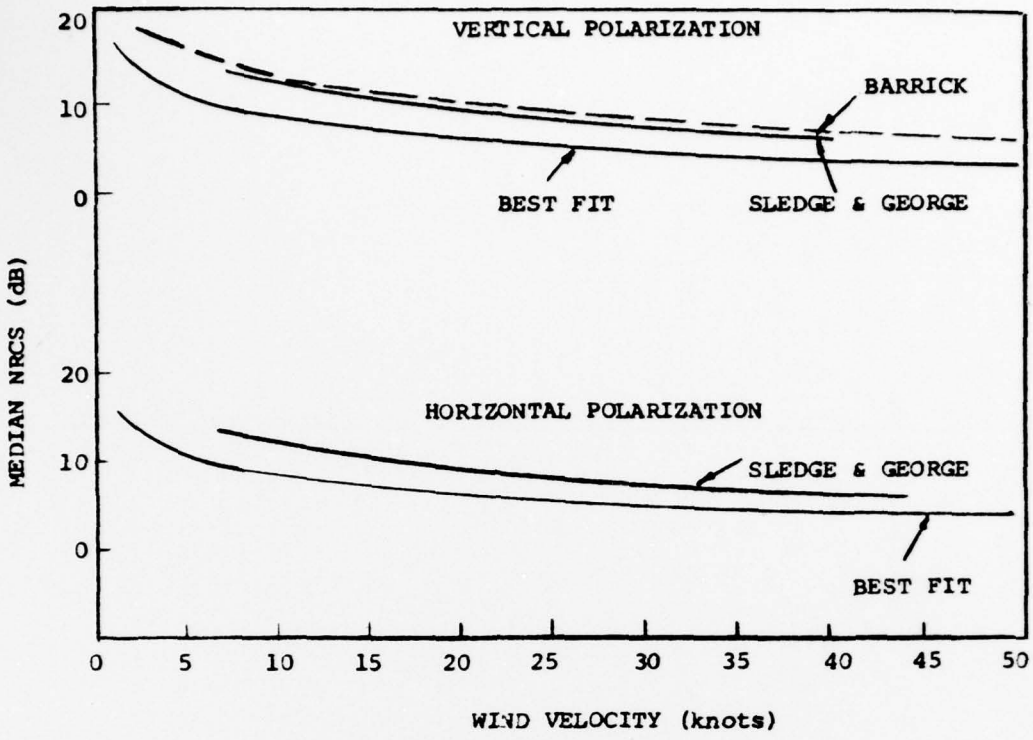

(a) Median NRCS vs wind velocity at vertical incidence, X band θ=90°

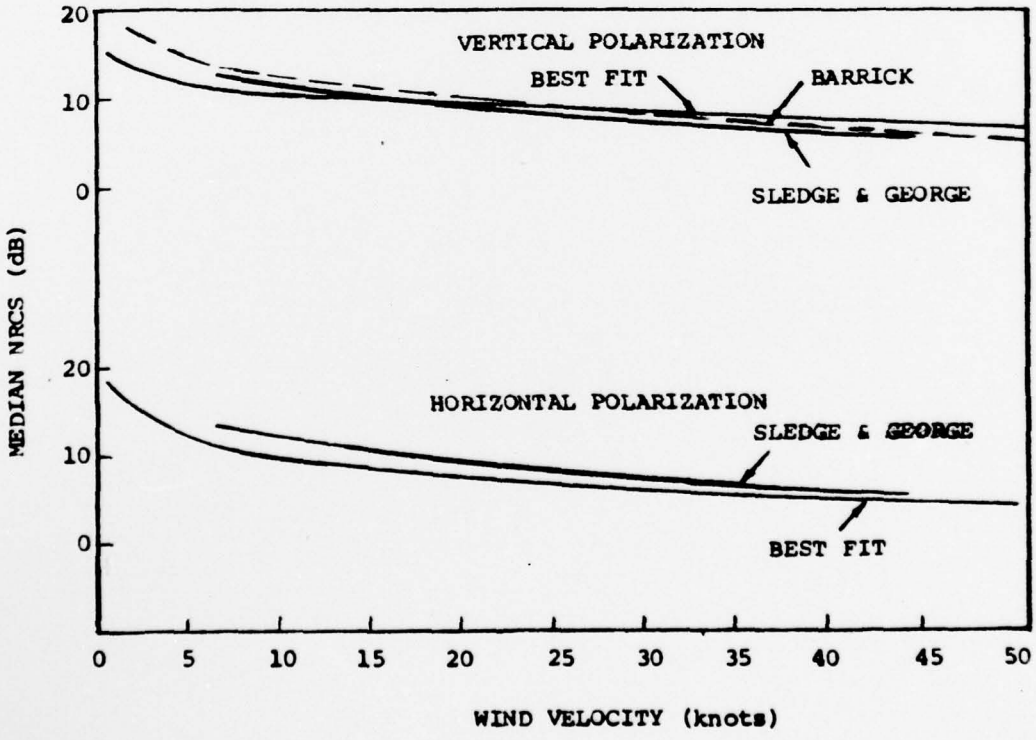

(b) Median NRCS vs wind velocity at vertical incidence, C band θ=90°

Figure 3. Median NRCS [12]

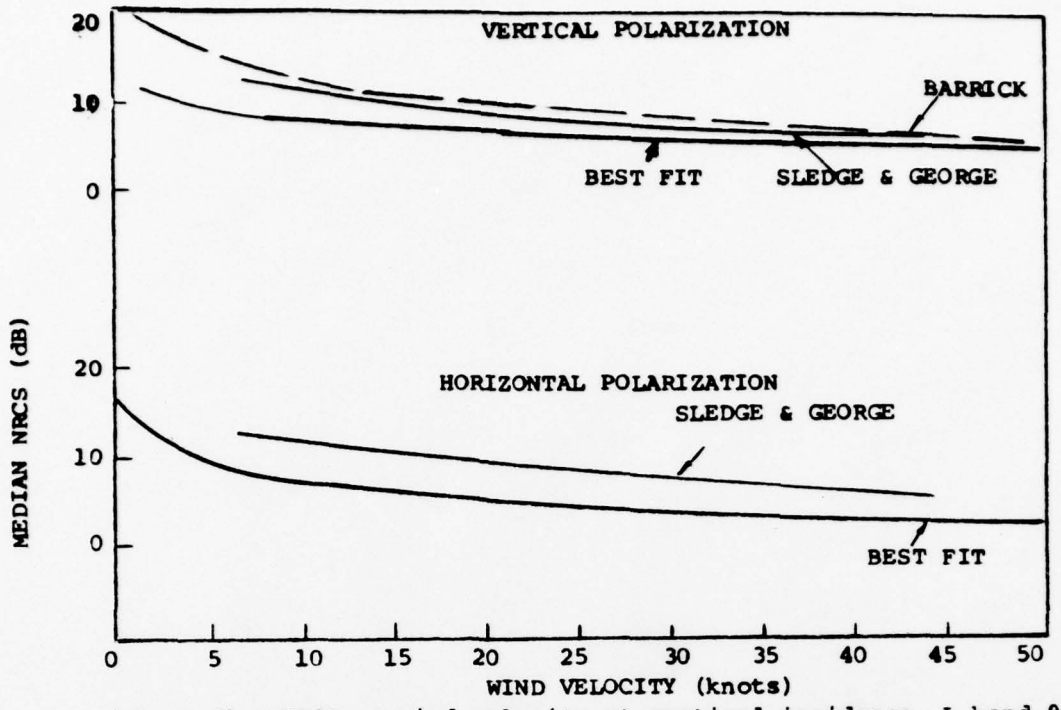

(c) Median NRCS vs wind velocity at vertical incidence, L band θ=90°

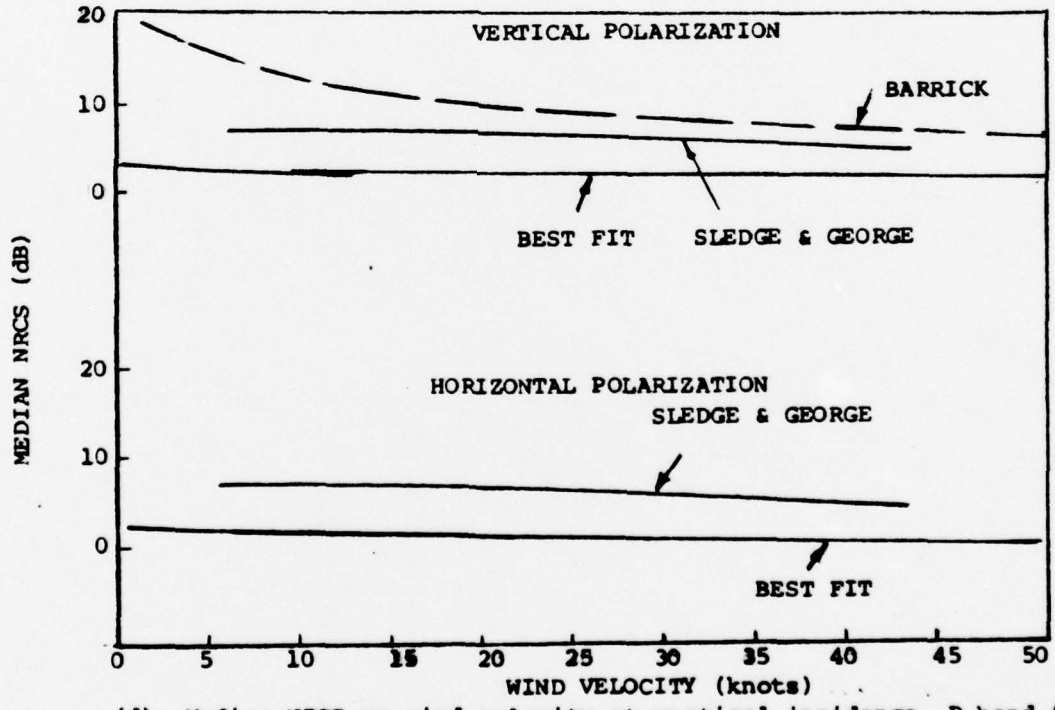

(d) Median NRCS vs wind velocity at vertical incidence, P band θ=90°

Figure 3. Median NRCS [12]

2.2 Conclusion

Barrick shows that as the frequency of operation is lowered from X band to L band the median NRCS decreases from 8 dB to 2 dB. At P band (428 MHz) the median NRCS is equal to the Fresnel power reflection coefficient. The implication is that the sea seems smooth for a monocycle pulse whose frequency content is less than 428 MHz even for winds up to 50 knots. This is not obvious and must be proven by experimentation.

If experimentation does not verify the surface is smooth for a monocycle pulse, the computer model will be modified by Daley's and Barrick's equation for the NRCS of a rough surface. The computer model is then more complex and the three regions defined by Skolnik will have to be accounted for.

SECTION 3

SINGLE FREQUENCY CALCULATIONS

3.1 Introduction

Single frequency calculations are made to determine what the frequency content of a monocycle should be for use in bathymetry and detection and identification of a salt water wedge. The calculations determine how much energy enters fresh water from the air, how much energy is reflected from and transmitted through a thermocline, and how much energy is reflected from a salt water wedge or bottom and returns to the air.

The radar range equation is modified to account for energy lost at each interface and for the attenuation of each medium. The influence of focusing is discussed. For a fresh water layer where the displacement current dominates propagation, it is permissible to account for losses in the layer by using the lossless forms of the solutions to Maxwell's equations and modifying them by the addition of the losses due to attenuation through the layer. [13] Appendix A shows that a negligible error occurs using this assumption when $\sigma \leq .01$ mhos/meter and a 16% error occurs when $\sigma = .1$ mhos/meter. The Maximum Allowable Attenuation (MAAT) is calculated using a Mininmum Discernible Signal (MDS) of -160 dBW. The advantage of this approach is that, if an MDS of -160 dBW is not realizable for the broadband monocycle pulse discussed in Section 4.3, the transmitted power and/or the antenna gain can be increased if the MDS must be decreased. For example, if the MDS is -120 dBW the transmitted power can be increased to +30 dBW and the antenna gain increased to 10 dB to compensate for the 40 dB of sensitivity lost. These

considerations become especially important if the bandwidth of the receiver is centered at 1 MHz. At this frequency atmospheric noise can reduce the lowest possible MDS from KTB equal 204 dB below one Joule by approximately 60 dB. [14] The lowest signal one could expect to detect in a one Hertz bandwidth would then be -144 dBW. If a 25% bandwidth is used (.75 MHz-1 MHz), the MDS is reduced to -90 dBW or 1 nanoVolt. It is shown that the Maximum Allowable Attenuation (MAAT) for a transmitted power of 1 Watt (0dB) and an antenna gain of 0dB the maximum allowable attenuation, after $1/R^2$ losses and interface losses are accounted for, is 110 dB.

3.2 Air/Water Interface

The air/water interface is the first return an airborne monocycle radar receives. This return is followed by a return from a thermocline, and then from the bottom or salt water wedge. The amount of power received depends on the frequency content and hence the shape of the transmitted pulse.

The dielectric constant of water is temperature and frequency dependent. Increasing the frequency or the temperature decreases the dielectric constant. Data taken from Von Hippel [15] show that the relative dielectric constant of water varies linearly from 87 to 55 as the temperature varies from 1.5° C to 95° C. This is valid for frequencies from 100 kHz to 300 MHz (see Figure 4). If the frequency is raised to 3 GHz the curve drops slightly and becomes curved. Increasing the frequency to 10 GHz or 25 GHz results in a drastic change in the curve of dielectric constant vs temperature.

The dependence of power reflected from the air/water interface on

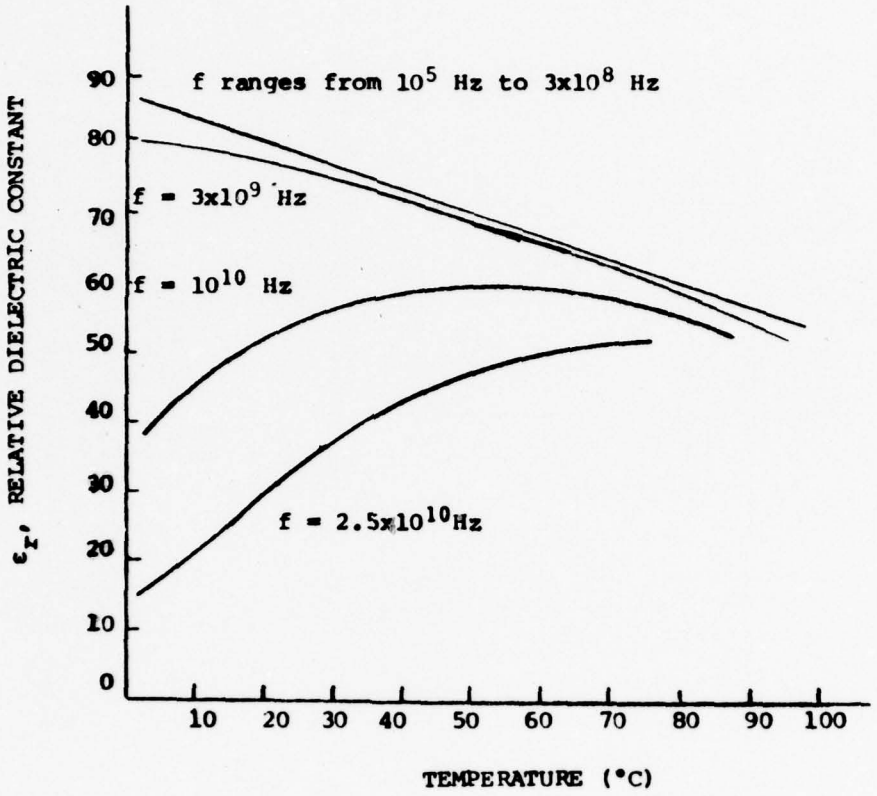

Figure 4. Relative dielectric constant of water vs temperature.[14]

dielectric constant is given by the following equations:

$$P_{aw} = P_t(\Gamma)^2 \triangleq P_t\{(\sqrt{\varepsilon_{fw}}-1)/(\sqrt{\varepsilon_{fw}}+1)\}^2 \quad (4)$$

when

$$\omega\varepsilon' >> \sigma \quad (5)$$

where

ω = $2\pi f$ = the angular frequency, radians/sec

f = frequency, Hertz

ε' = the dielectric constant of the material being investigated, Farad/meter

σ = the conductivity of the material being investigated, mhos/meter

ε_{fw} = the relative dielectric constant of water

Γ = the Fresnel reflection coefficient for normal incidence at the air/fresh water interface

P_{aw} = power reflected from the air/water interface, Watts

P_t = transmitted power, Watts

If it is assumed that 10kW is transmitted and that the relative dielectric constant of water is 79, the power reflected from the air/water interface is

$$P_{aw} = P_t\{(\sqrt{79}-1)/(\sqrt{79}+1)\}^2 = 10 \text{ kW } (.798)^2$$

$$= 6.36 \text{ kW} \quad (6)$$

The power transmitted into the water is the difference between the total power and the power reflected at the interface:

$$P_{wi} = P_t - P_{aw} = 3.64 \text{ kW} \tag{7}$$

At the air/fresh water interface, 63.6% of the energy is reflected. This is a one-way transmission loss through the interface of 4.4 dB.

3.3 Thermocline Interface

In relatively stagnant water the temperature changes with depth. This change represents a discontinuity in the dielectric constant and a reflection occurs. Figure 5 presents depth vs temperature for Lake Erie.[16] Although this data is not directly applicable to estuaries, an indication of what happens to electromagnetic energy at a thermocline interface is obtained. The temperature at the surface of the lake is 73°F (22.78°C). At a depth of 60 feet (18.29 meters) the temperature is 50°F (10°C). From Figure 4, the dielectric constants for the above temperatures are $\varepsilon_{w1} = 79$ and $\varepsilon_{w2} = 83.5$, respectively.

The power reflected from the thermocline is equal to the power in the water times the lower reflection coefficient of the thermocline:

$$P_{th} = P_{wi}(\Gamma_{th})^2 = P_{wi}\{(\sqrt{\varepsilon_{w2}/\varepsilon_{w2}}-1)/(\sqrt{\varepsilon_{w2}/\varepsilon_{w1}}+1)\}^2 \tag{8}$$

where

P_{th} = power reflected from the thermocline

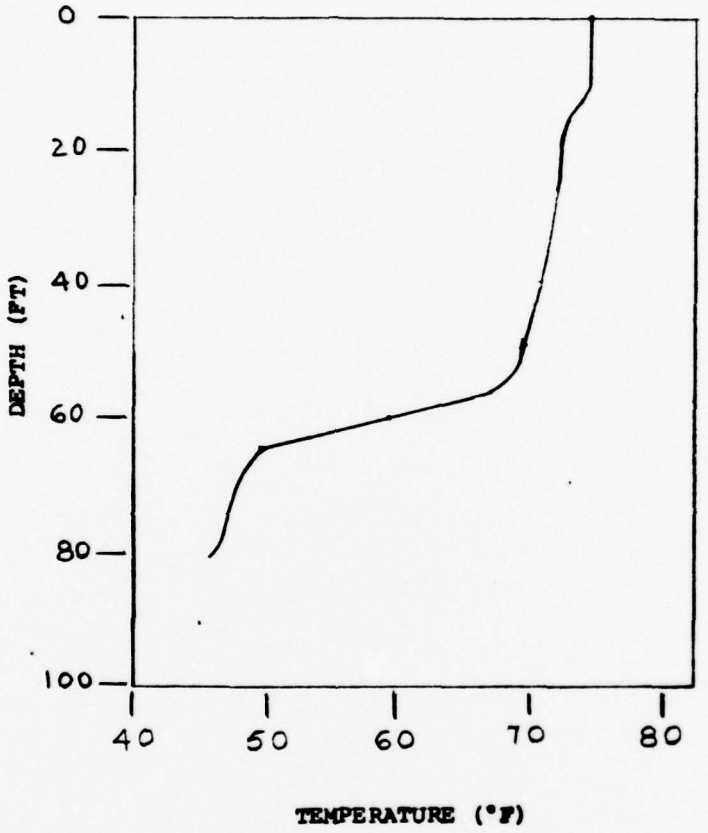

Figure 5. Bathythermograph temperature recordings in the central basin of Lake Erie. [16]

$(\Gamma_{th})^2$ = Fresnel power reflection coefficient at the thermocline

Substituting equation (7) and the values of dielectric constant ε_{w1} and ε_{w2} into equation (8) and accounting once more for the water air interface, it can be shown that the power transmitted back from the thermocline into the air is .254 Watts. In a similar manner it can be shown that if the frequency is increased to 10 GHz, the power transmitted back into the air is 3.83 Watts. If the frequency is increased to 25 GHz, the power transmitted back into the air is 28.4 Watts. As will be shown, the return from the salt water interfaces at the frequencies to be used is much larger than these values. Therefore, thermoclines do not interfere with the detection of salt water wedges.

3.4 Salt Water Interface

It is assumed that a horizontal salt water wedge with a relative dielectric constant of 80 and a conductivity equal to 4 mhos/meter exists under a fresh water layer with relative dielectric constant equal to 83.5 and zero conductivity. Since the conductivity dominates at the salt water wedge, the power reflection coefficient at this interface is written

$$\Gamma_{sw}^2 = \{(\eta_3/\eta_2)-1\}/\{(\eta_3/\eta_2)+1\} \qquad (9)$$

where

η_3 = the complex characteristic wave impedance for uniform plane waves in the salt water wedge, Ohms

η_2 = the complex characteristic wave impedance for uniform plane waves in the fresh water, Ohms

It can be shown that

$$\eta_3 \doteq (\omega\mu/2\sigma)^{1/2} \tag{10}$$

and

$$\eta_2 \doteq (\mu/\varepsilon'_{w2})^{1/2} \tag{11}$$

where

$$\varepsilon'_{w2} = \varepsilon_{w2}\,\varepsilon_o$$

and

ε_o = the dielectric constant of free space

= 8.854×10^{-12} Farad/meter

The power reflection coefficient for salt water calculated by substituting equations (10) and (11) into (9) is presented in Table I. The power that is transmitted through the thermocline to the salt water is the power in the fresh water, P_{wi}, minus the power reflected from the thermocline, P_{th}. In the frequency range 10^5 to 3×10^8 Hz, this power is 3.64 kWatts. Using the power reflection coefficients in Table I, the power returned to the thermocline from the salt water interface can be calculated. The power that enters the air can also be calculated and is presented in Table I.

3.5 Attenuation of Plane Electromagnetic Waves

In the above discussion the losses due to the conductivity of the water are neglected. The characteristic impedance η_2 is therefore independent of the conductivity, σ. This is consistent with the initial statement in

TABLE I

The power that returns to the monocycle radar, P_{air}, after it has travelled through a thermocline in fresh water and is reflected from a salt water layer.

f (Hz)	Γ^2_{sw}	P_{sw}(kW)	P_{air}(kW)
10^5	.97	3.53	1.28
10^6	.91	3.31	1.21
10^7	.74	2.69	.98
10^8	.37	1.35	.49

where,

Γ_{sw} = The Fresnel reflection coefficient of the salt water

P_{sw} = The power reflected from the salt water

P_{air} = The power in air at the monocycle radar

and the constitutive parameters are:

a. Upper layer of the thermocline, $\epsilon_{w1} = 79$ and $\sigma = 0$ mhos/meter

b. Lower layer of the thermocline, $\epsilon_{w2} = 83.5$ and $\sigma = 0$ mhos/meter

c. Salt water, $\epsilon_{sw} = 80$ and $\sigma_{sw} = 4$ mhos/meter

the approach that the losses are separated so that their individual contribution to the problem can be properly evaluated. Instead of using a complex form for η_2, the attenuation in dB per meter is calculated for various conductivities. In Section 4, the computer model does not use any approximations and considers both η_2 and η_3 to be complex. The conductivity is related to the relative dielectric constant and loss tangent of a material by the following formula: [17]

$$\sigma = f\,\varepsilon_r \tan\delta / 1.8\times10^{10} \text{ mhos/meter} \qquad (12)$$

where

f = frequency in Hertz

ε_r = relative dielectric constant

$\tan\delta$ = loss tangent = conduction current divided by displacement current

It is shown in Appendix A that the units of equation (12) are mhos/meter. The attenuation constant is related to the relative dielectric constant and loss tangent by the following formula: [18]

$$\alpha = \{2\pi(\varepsilon_r)^{1/2} / \lambda_1\}\{\{(1+\tan^2\delta)^{1/2} - 1\}/2\}^{1/2} \qquad (13)$$

where

λ_1 = free space wavelength

The loss in dB/meter is obtained by multiplying equation (13) by 8.68. The

dependence of α on σ is given by equation (20) in Section 4.2. Using equations (12) and (13) tables of attenuation versus depth are constructed. Tables IIa through c present depth of penetration in meters versus attenuation for distilled water. The conductivity of distilled water is frequency dependent and therefore varies in the Tables.[19] The depth of penetration varies from 1 km to 20 meters and the two-way attenuation varies from 74 dB to 155 dB. Depth of penetration vs attenuation for different values of conductivity and for the frequency range 25 MHz to 500 MHz is presented in Table III. The attenuation increases rapidly with conductivity. When the conductivity is .001 mhos/meter, the one-way attenuation is 9.15 dB. If the conductivity is increased to .005 and .01 mhos/meter the one-way attenuation is 45.7 dB and 83.5 dB, respectively. Increasing the conductivity to .1 mhos/meter results in a one-way attenuation of 181.7 dB after 10 meters. This is prohibitively large and is the cutoff conductivity for frequencies in the range 25 to 500 MHz.

The conductivities of some natural bodies of water obtained from the Waterways Experiment Station [20] are:

1. The Mississippi has a conductivity of .02 mhos/meter
2. Hudson Bay has a conductivity of .2 mhos/meter
3. Industrial waters have conductivities ranging from .05 to .1 mhos/meter.

Typical values of conductivity for areas in the Baltic Sea range from .8 to 1.2 mhos/meter. [21]

To be able to detect a salt water wedge beneath a "fresh water" layer whose conductivity is .1 mho/meter or higher, it is necessary to lower the

TABLE IIa

Attenuation vs depth for distilled water [19]

(a) $T = 25°C$, $f = 10^7$Hz, $\epsilon_{fw} = 78.2$, $\tan\delta = 46\times10^{-4}$, $\sigma_{fw} = 2\times10^{-4}$ mhos/meter, $\alpha = .00427$ (meter)$^{-1}$, $8.68\,\alpha = .037$ dB/meter.

d (meters)	One-Way Attenuation (dB)	Two-Way Attenuation (dB)
10	.37	.74
20	.74	1.48
30	1.11	2.22
40	1.48	2.96
50	1.85	.37
100	3.7	7.4
500	18.5	37.0
1,000	37.0	74.0

TABLE IIb

Attenuation vs depth for distilled water [19]

(b) $T = 25°C$, $f = 10^8$ Hz, $\tan\delta = 50\times10^{-4}$, $\varepsilon_{fw} = 78$, $\alpha_{fw} = 21.81\times10^{-4}$ mhos/meter, $\alpha = .0463$ (meter)$^{-1}$, $8.68\,\alpha = .403$ dB/meter.

d (meters)	One-Way Attenuation (dB)	Two-Way Attenuation (dB)
10	4.03	8.06
20	8.06	16.12
30	12.09	24.18
40	16.12	32.24
50	20.15	40.30
100	40.3	80.60
200	80.6	161.2

TABLE IIc

Attenuation vs depth for distilled water [19]

(c) $T = 25°C$, $f = 3 \times 10^8$ Hz, $\tan\delta = 160 \times 10^{-4}$, $\varepsilon_{fw} = 77.5$, $\sigma_{fw} = 2.09 \times 10^{-2}$ mhos/meter, $\alpha = .4453$ (meter)$^{-1}$ 8.68 $\alpha = 3.865$ dB/meter.

d (meter)	One-Way Attenuation (dB)	Two-Way Attenuation (dB)
2	7.73	15.46
4	15.46	30.92
6	23.19	46.38
8	30.92	61.84
10	38.65	77.30
20	77.30	154.60

TABLE III

One-Way Attenuation vs Depth For 25 MHz <f< 500 MHz

σ_{fw} (mhos/m)	.001	.005	.01	.1
8.68α(dB/m)	.18	.91	1.82	18.17
d (m)	Attenuation (dB)			
1	.18	.91	1.82	18.17
10	1.82	9.14	18.27	181.7
30	5.48	27.43	54.81	
40	7.31	36.58	73.08	
50	9.14	45.73	83.54	
60	10.97	54.87	109.62	
70	12.80	64.02		
80	14.63	73.16		
90	16.46	82.31		
100	18.29	91.46		

where

$\varepsilon_{fw} = 80$

frequency content of the monocycle pulse below 25 MHz. If the highest frequency component of the monocycle pulse is low the antenna needed to support such a monocycle pulse becomes large. If the antenna is placed on the water the problem becomes easier to solve. This serves two purposes. The reflection at the air water interface, which becomes larger as the frequency content of the monocycle pulse is lowered, is eliminated, and the water loads the antenna. King states [22] that an antenna loaded by sea water is electrically 50 times longer than the same antenna in air. The implication is that when conductivity of the fresh water layer is greater than .1 mho/meter the propagation is dominated by the conductivity and the loading factor although not as high as sea water (50) is greater than that of fresh water (9). The antenna if placed on the fresh water whose conductivity is greater than .1 mho/meter does not have to be as large as the same antenna in air. This is a concept that remains to be proven.

Table IV is a list of losses incurred for a monocycle radar 30 meters above the fresh water layer. The constitutive parameters for the fresh water are $\varepsilon_r = 80$ and σ ranges from .001 to .01 mhos/meter. For the salt water, $\varepsilon_r = 80$ and $\sigma = 4$ mhos/meter. The MAAT for a transmitted power of 1 Watt (0dB) and an antenna gain of 0dB is approximately 110 dB. The table contains the effect of a rough surface even though the surface appears smooth for a pulse whose frequency content is below 428 MHz. The losses due to the thermocline are negligible. The losses due to the air/water, thermocline and salt interface are less than 20 dB. The total losses including $1/R^2$ and rough surface losses are approximately 50 dB. The table is important because it puts the losses in their proper prospective.

TABLE IV

Maximum Allowable Attenuation (MAAT) With The Monocycle Radar 15 Meters Above The Fresh Water

f(MHz)	25	50	100	200	300	400	500
P_t(dBW)	0	0	0	0	0	0	0
T_1(dB)	4.42	4.42	4.42	4.42	4.42	4.42	4.42
$T_2(10^{-4}$dB)	8.68	8.68	8.68	8.68	8.68	8.68	8.68
Γ^2_{sw}(dB)	2.06	2.92	4.17	5.99	7.42	8.66	9.76
$T_2(10^{-4}$dB)	8.68	8.68	8.68	8.68	8.68	8.68	8.68
T_1(dB)	4.42	4.42	4.42	4.42	4.42	4.42	4.42
Subtotal	10.9	11.76	13.01	14.83	16.26	17.5	18.6
R.S.(dB)	5.0	5.0	5.0	5.0	5.0	5.0	5.0
$1/R^2$(dB)	29.5	29.5	29.5	29.5	29.5	29.5	29.5
G (dB)	0	0	0	0	0	0	0
Subtotal 2	45.4	46.26	47.51	49.33	50.76	52	53.1
MDS (dBW)	160	160	160	160	160	160	160
MAAT	114.6	113.7	112.5	100.7	109.2	108	106.9

where,

R.S. = effect of rough surface
MDS = minimum discernible signal

and the constitutive parameters are:

a. Fresh water layer $\epsilon_{w1} = 80$ and $.001 \leq \sigma \leq .01$ mhos/meter

3.6 Radar Range Equation

The presentation given in Section 3.4 is one approach to finding the limitations of using a radar in bathymetry. Another approach is to modify the radar range equation so that propagation through various media is expressed explicitly.

"The surface of the sea may be considered as composed of a number of individual scatters which scatter or reflect the incident radar energy independent of one another. The average echo signal (average over many radar sweeps) from all independent scatters illuminated by the antenna beam is

$$\bar{P}_r = \{(P_t G^2 \lambda^2)/(4\pi)^3 R^4\} \Sigma_i \bar{\sigma}_i \qquad (14)$$

where $\bar{\sigma}_i$ is the time average radar cross section of the i^{th} scatter". [23] Since the estuary and the interfaces beneath it present an extended target the radar range equation becomes

$$\bar{P}_r = P_t G^2 \lambda_l^2 \theta_\beta \phi_\beta \sigma^\circ / (4\pi)^3 R_l^2 \sin\phi \qquad (15)$$

where

P_t = transmitted power

G = antenna gain

λ_l = wavelength in free space

θ_β = 3dB beamwidth in "azimuth"

ϕ_β = 3dB beamwidth in "elevation"

σ° = NRCS

R_1 = height of the radar above the fresh water interface

ϕ = depression angle ($\phi = 0°$ on the horizon)

To include transmission through materials and reflections from interfaces of materials, the radar range equation must be modified to include the energy lost from reflections at each interface. It must also include losses due to conductivity of the materials and it must account for the focusing effect the electromagnetic energy receives when it is refracted at each interface. For normal incidence equation (15) takes the following form:

$$P_r = \{P_t G^2 \Gamma_{sw}^2 T_1^4 T_2^4 \theta_\beta \phi_\beta \lambda_1^2 / (4\pi)^3 R_1^2\} \exp(-2\alpha_2 R_2 - 2\alpha_2' R_2') \qquad (16)$$

where

R_1 = height of radar above the fresh water interface

R_2 = range in upper layer of thermocline in fresh water

R_2' = range in lower layer of thermocline in fresh water

Γ_{sw} = Fresnel reflection coefficient of salt water

α_2 = the attenuation in upper layer of thermocline in fresh water

α_2' = the attenuation in lower layer of thermocline in fresh water

T_1 = the Fresnel transmission coefficient at the air/fresh water interface

T_2 = the Fresnel transmission coefficient at the thermocline interface

Equation (16) is derived for transmission through three media: Air, the upper layer of the thermocline and the lower layer of the thermocline. The desired target is the salt water interface, Γ_{sw}. It is readily extended to more media by multiplying by the transmission coefficient raised to the 4th power for losses at interfaces and by adding attenuation coefficients to the exponent to account for dissipative losses. It is assumed that a single frequency plane wave is normally incident on all boundaries and that the attenuation of the media make the amplitude of the second and higher bounces between media negligible. The desired reflection is the first return from medium 3. Focusing is accounted for by assuming there are no $1/R^2$ loss in the media. Using a relative dielectric constant of water of 79 and Snell's law, it can be shown that an antenna pattern with a half power beamwidth of 60° is "focused" to 5.44°. A 5° half power beamwidth is "focused" to .56°.

Equation (16) has been computer programmed and an analysis is performed to determine the depth of penetration for an airborne monocycle radar. The radar is assumed to be 15 meters above a fresh water layer over a salt water wedge. In the programming, the following values (or magnitudes) have been given to the parameters in equation (16):

P_t = 0dBW

G = 8.75 dB

$\theta_\beta = \phi_\beta$ = 60 degrees

R_1 = 15 meters

R_2 = variable to be determined

R'_2 = 0

Γ_{sw} = Fresnel reflection coefficient of salt water at a particular frequency

T_1 = Fresnel transmission coefficient of air/fresh water interface which is a variable depending on frequency and conductivity of the fresh water layer

T_2 = 1

α'_2 = 0

α_2 = Attenuation calculated for various conductivities

λ_1 = Wavelength of particular frequency being considered in free space

Table V presents depth of penetration for 10 MHz, and 500 MHz. The Table has three major headings:

1. f (MHz)
2. σ_{fw} (mhos/meter)
3. d (meters)

The d (meters) heading is broken down into two subheadings. P_t is the transmitted power and the depth in meters for 0 dBW and 43 dBW is given. The column with the heading E_{loss} represents the increase in power obtained by integrating 1000 pulses with an integration loss of 10 dB. At 10 MHz the minimum discernable signals are considered, 110 dB and 160 dB. At 10 MHz the maximum depth of penetration when the conductivity is .1 mhos/meter is 7 meters. At 100 MHz the maximum depth is 5 meters and at 500 MHz the maximum depth is 4.4 meters.

TABLE V

Depth of penetration d (meters), vs conductivity, σ(mhos/meter), for a fresh water layer over salt water, with the radar 15 meters above the fresh water, for frequencies f (MHz).

f(MHz)	σ_{fw}(mhos/meter)	d (meters)					
		P_t = 0dBW		P_t = 43 dBW		nE$_{loss}$ = 20 dB	
		MDS		MDS		MDS	
		110	160	110	160	110	160
10	.001	248	385	366	501	421	557
	.005	50	77	73	101	84	112
	.01	25	39	37	51	42	56
	.1	3	4.8	4.6	6.4	5.3	7.1
100	.001	186	322	303	440	358	495
	.005	37	65	61	88	72	99
	.01	19	32	30	44	36	50
	.1	1.9	3.2	3.0	4.4	3.6	4.9
500	.001	132	269	250	386	304	441
	.005	26	54	50	77	61	88
	.01	13	27	25	39	30	44
	.1	1.3	2.7	2.5	3.9	3.0	4.4

*where:

MDS = Minimum Discernible Signal

n = The number of pulses integrated (assumed to be 1000)

E_{loss} = Integration loss (assumed to be -10dB)

and the constitutive parameters are:

a. Fresh water ε_{fw} = 80, .001 $\leq \sigma_{fw} \leq$ .1 mhos/meter

b. Salt water ε_{sw} = 80 σ_{sw} = 4 mhos/meter

The single frequency analysis using equation (16) shows that decreasing the frequency increases depth of penetration. As originally explained in paragraph 1.3, Approach, the single frequencies or harmonic waves will be Fourier transformed from the frequency domain into the time domain to form a monocycle pulse. If the desired depth of penetration is greater than 7 meters a monocycle pulse whose frequency content is lower than 10 MHz should be used.

Decreasing the frequency content of the monocycle pulse to increase depth of penetration as the conductivity of the fresh water layer is increased above .1 mhos/meter, implies a longer pulse and an increase in reflected energy from the air/fresh water interface. The increase in reflected energy is undesirable. A monocycle pulse whose frequency content is less than 10 MHz will be approximately 30.5 m long in air. By placing the antenna on the water, or within a few feet of it, the size of the antenna can be reduced by the loading effect of the water. The antenna is loaded by the water because propagation of electromagnetic energy is slowed down making the antenna electrically longer. If the displacement current is much greater than the conduction current, the antenna will seem electrically longer by the square root of the dielectric constant. For the case under consideration, that is, the frequency content of the monocycle pulse is less than 10 MHz and the conductivity of the fresh water is greater than .1 mhos/meter, the conduction current dominates propagation. The electromagnetic energy propagates more slowly than before and the 30.5 m antenna is electrically longer than it was when the displacement current dominated propagation.

To have an equivalent directivity of a 30.5 m (100 ft) antenna in air, an antenna on a fresh water layer where propagation is dominated by the displacement current need be only 3.4 m (11.1 ft) long. For the case where the conduction current dominates propagation it is hypothesized that the antenna need be less than 3.4 m (11.1 ft) long to obtain the same directivity. King showed [24] that when the conductivity is 4 mhos/meter and the frequency is 1.4 MHz the electrical size of the antenna is increased by a factor of 50. When the conductivity is greater than .1 mhos/meter the electrical length of the antenna will be between 9 and 50 times greater than it is in air. Increasing the electrical length of an antenna increases its directivity. Placing the antenna on, or close to, the water eliminates the $1/R_1^2$ loss and the T_1^4 loss in equation (16).

The focusing effect caused by the air/water interface is lost. The focusing collimated the beam and eliminated $1/R_2^2$ losses in the water. The $1/R_2^2$ loss in the water is taken into account by letting $R_1 = R_2$. The transmission loss at the air/water interface does not exist, therefore, $T_1 = 1$. The radar range equation is rewritten for the antenna on the water as follows:

$$P_r = \{P_t G^2 \Gamma_{sw}^2 \theta_\beta \phi_\beta \lambda_w^2 \exp(-2\alpha_2 R_2)\}/(4\pi)^3 R_2^2 \qquad (17)$$

where in equation (16) for the antenna on the water:

$T_1 = 1$

$T_2 = 1$

$\lambda_1^2 = \lambda_w^2$

λ_w = wavelength in the water

$$\alpha'_2 = 0$$

$$R_1^2 = R_2^2$$

$$R'_2 = 0$$

Although the effect of refraction is missing, the antenna is now "loaded" by the water making it electrically longer. This is similar to focusing because the gain of the antenna increases and the beamwidth becomes narrower. In programming the problem under consideration, when the antenna is placed on the water the gain is kept the same as when it is in the air. This is interpreted as decreasing the size of the antenna. In other words, if the antenna is kept the same size on the water as it is in the air, the parameter of gain in the computer program would have to be increased. This would in effect focus the energy, so that focusing exists regardless of whether the antenna is on or off the water.

Table VI presents the depth at which a salt water wedge can be detected for varying conductivities of the fresh water layer when the antenna is on the water. Three frequencies are shown, 10 MHz, 100 MHz and 500 MHz. The d (meters) column is subdivided into 5 columns containing minimum discernible signals that vary from -80 dBW to -160 dBW. At 10 MHz, with a conductivity of .1 mhos/meter, a salt water wedge can be detected approximately 5 meters below the surface. If the frequency is decreased the depth at which a salt water wedge can be detected is increased. Table VII gives the depth at which a salt water wedge can be detected when the frequency is 1, 2, 3, 4 and 5 MHz. At 1 MHz, when the conductivity is .1 mhos/meter, a salt water wedge can be detected approximately 15 meters below the surface. Doubling the conductivity

TABLE VI

Depth, d(meters), at which a salt water layer can be detected when a fresh water layer with various values of conductivity, σ_{fw} (mhos/meter), is over it, for frequencies, f = 10, 100 & 500 MHz. The antenna is on the water, P_t = 0 dBW & G = 8.75 dB.

f(MHz)	σ_{fw}(mhos/meter)	d(meters)				
		MDS (dBW)				
		-80	-100	-120	-140	-160
10	.001	203	257	312	367	421
	.005	41	52	63	73	84
	.01	20	26	31	37	42
	.1	2.6	3.3	4.1	4.8	5.5
	1.0	.62	..80	.99	1.2	1.4
100	.001	140	195	250	304	359
	.005	28	39	50	61	72
	.01	14	19	25	30	36
	.1	1.4	1.9	2.5	3.0	3.6
	1.0	.16	.24	.31	.38	.45
500	.001	87	141	196	251	305
	.005	17	28	39	50	61
	.01	8.7	14	20	25	31
	.1	.9	1.4	1.9	2.5	3.1

*where,

MDS = Minimum Discernible Signal and varies from -80 to -160 dBW.

TABLE VII

Depth, d(meters), at which a salt water layer can be detected when a fresh water layer with various values of conductivity, σ_{fw} (mhos/meter), is over it, for frequencies, f = 1,2,3,4.& 5 MHz. The antenna is on the water, P_t = 0 dBW & G = 8.75 dB.

f(MHz)	σ_{fw}(mhos/meter)	d(meters)				
		MDS (dBW)				
		-80	-100	-120	-140	-160
1	.01	34	41	48	56	63
2		27	33	39	45	51
3		25	30	36	42	49
4		23	29	35	40	46
5		22	28	34	39	45
1	.1	9	11	12	14	16
2		6	7	9	10	11
3		5	6	7	8	9
4		4	5	6	7	8
5		3.6	4.5	5.4	6.3	7.2
1	.2	6	7	9	10	11
2		4	5	6	7	8
3		3	4	5	5.5	6.3
4		2.7	3.4	4	4.7	5.4
5		2.4	3	3.6	4.2	4.8

Where,

MDS = Minimum Discernible Signal and varies from -80 to -160 dBW.

MDS = P_r in equation (17)

to .2 mhos/meter reduces the depth at which a salt water wedge can be detected at this frequency to approximately 10 meters.

Table VI and VII are important because they give the radar design engineer a range of frequencies that a monocycle pulse should consist of to detect a salt water wedge. For example, if the salt water wedge is 14 meters below a fresh water layer whose conductivity is .1 mhos/meter the frequency content of the pulse should be less than 1 MHz. With a transmitter power of 0 dBW and an antenna gain of 8.75 dB, the sensitivity of the receiver must be -140 dBW. The radar engineer can also decide from Tables VI and VII what bandwidth the receiver should have so that the return monocycle pulse will be undistorted and the signal to noise ratio (SNR) maximized. For example, if the upper limit of the receive bandwidth is greater than the highest frequency of the return signal, unwanted noise will enter the radar degrading the SNR. Assume that the antenna limits the lower frequency components of the transmitted monocycle pulse. If the lower limit of the receiver is higher than the lowest component received it will distort the return pulse. If it is unnecessarily lower than the lowest component transmitted more noise will enter the receiver further degrading the SNR.

The computer model is used to calculate the ratio of received power to transmitted power. These results are plotted in Figure 6. In the computer model the height of the radar above the fresh water is 15 meters. The depth of the fresh water is 10 meters, the constitutive parameters of the fresh water are σ = .001 mhos/meter and ϵ_r = 80. The constitutive parameters of the salt water are σ = 4 mhos/meter and ϵ_r = 80. The results in Figure 6

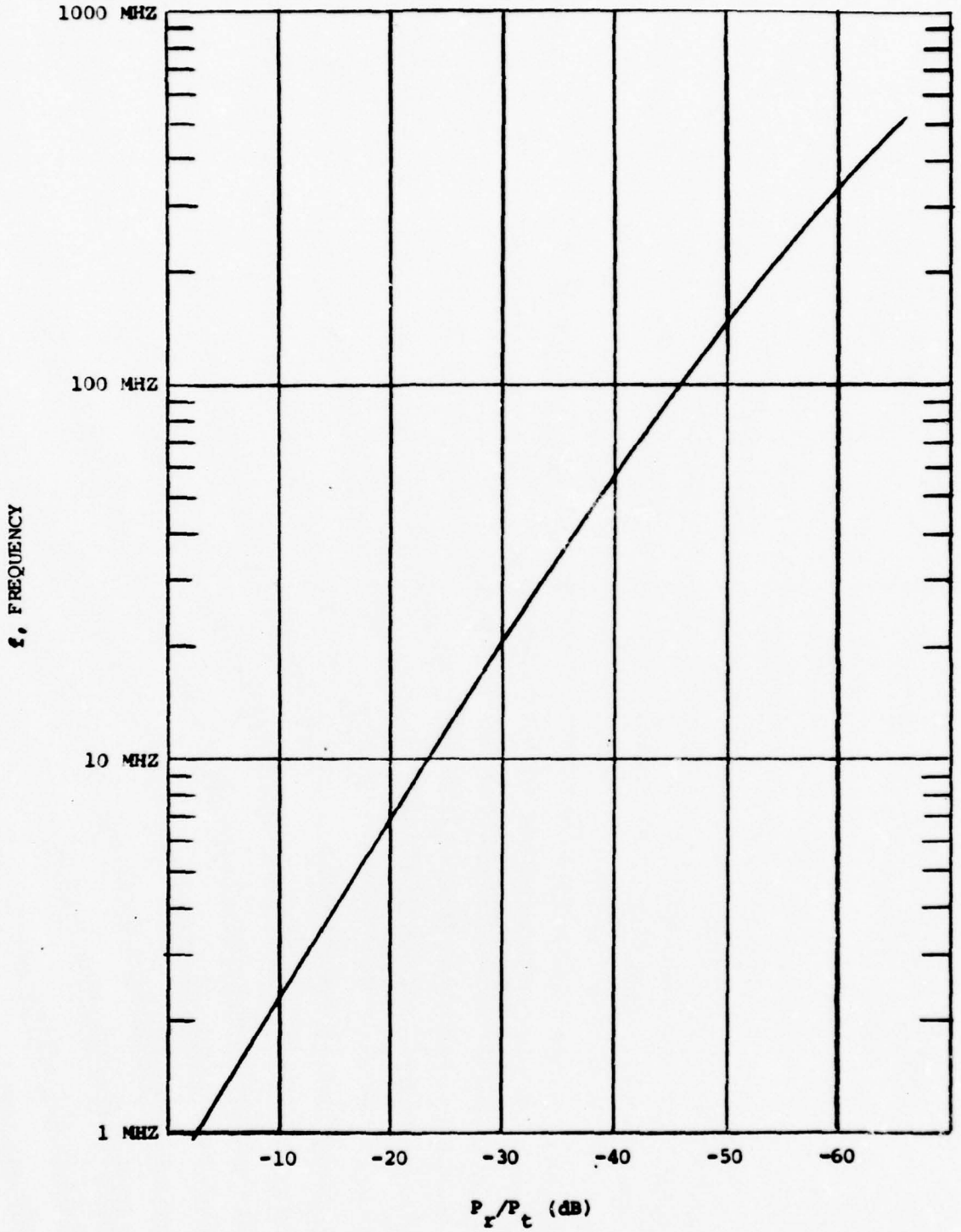

Figure 6. Frequency vs normalized received power.

show that the frequency is increased from 1 MHz to 500 MHz the normalized received power decreases from -2.1 dB to -65.3 dB. These results show that as the frequency content of the monocycle pulse is lowered the ratio of received power to transmit power increases and the depth at which a salt water wedge can be detected increases.

To determine the effect of changes in conductivity and dielectric constant on returned power using equation (16) without a themocline the computer model in Figure 7 is evaluated with the following parameters:

1. The radar height in air above the fresh water layer is, $R_1 = 15$ meters. The frequency is 1 MHz and the depth of the fresh water is 1 meter.

2. The constitutive parameters are:

(a) $\varepsilon_1 = 1$ $\sigma_1 = 0$ mhos/meter (air)

(b) $\varepsilon_2 = 80$ $\sigma_2 = .001$ mhos/meter (fresh water)

(c) $\varepsilon_3 = 80$ $\sigma_3 = 4$ mhos/meter (fresh water)

For these conditions the ratio of received power to transmit power, P_r/P_t, equals +1.2 dB. Changing the conductivity of the fresh water from .001 to .1 mhos/meter results in a ratio of received power to transmit power of -26.1 dB. The results show that depth of penetration depends greatly on the conductivity of the fresh water layer. To determine the sensitivity to changes in dielectric constant the ratio of received power to transmit power is calculated for the following constitutive parameters:

(a) $\varepsilon_1 = 1$ $\sigma_1 = 0$ mhos/meter

(b) $\varepsilon_2 = 80$ $\sigma_2 = .001$ mhos/meter

(c) $\varepsilon_3 = 74$ $\sigma_3 = .001$ mhos/meter

For these conditions the ratio of received power to transmit power is -36 dB. Changing ε_3 to 70, with σ_3 constant at .001 mhos/meter, the ratio of received power to transmit power is -31.4 dB. Changing the dielectric constant of the third layer from 74 to 70 results in a change of P_r/P_t of 4.6 dB. At this time the calculations have not been performed with the constitutive parameters of the second layer constant and only the conductivity of the third layer changed. The results show that a monocycle pulse can detect minute changes in dielectric constant and is very sensitive to conductivity.

3.7 Conclusion

The single frequency analysis shows that it is possible to detect a salt water wedge using an airborne monocycle radar. The analysis shows that, in the frequency range from 25 MHz to 500 MHz, 4.42 dB is lost at the air/fresh water interface. This does not present a significant systems problem. The loss at the thermocline is negligible and the surface is smooth for winds up to 50 knots. These results had to be calculated because they are not obvious and it was necessary to demonstrate that they do not seriously impair a monocycle radar's operation in bathymetry.

The modified range equation shows explicitly how the received power depends on the reflection coefficient of the desired interface and on the transmission coefficients of the undesired interface. It implicitly shows a focusing effect by the absence of $1/R^2$ losses in the fresh water. Focusing becomes greater every time an interface is penetrated. This result is important because losses in air ($1/R^2$ losses) can be minimized by placing the

antenna close to the air/fresh water interface and focusing can be taken advantage of. The $1/R^2$ losses are thereby minimized in the fresh water. When the energy passes through the interface in the opposite direction the energy is defocused but for the model of air/fresh water and salt water being analyzed a decisive advantage is gained.

The results can be extended to other materials by changing the values of Γ_{sw}, α_2, α_2', T_1 and T_2 in equation (16). These parameters change because they are functions of the dielectric constant and conductivity, which change for different materials. Appendix B shows that for dry earth 80% of the energy transmitted enters dry earth, and 97% enters trees. It is shown in Appendix B that it may be feasible to detect fresh water under 3.7 km of glacial ice. Table B1 presents the ratio of received power to transmit power, P_r/P_t, for harmonic components of a 2 ns monocycle pulse.

In Appendix C it is shown neglecting the losses in calculating the characteristic impedance for a fresh water layer whose conductivity is less than at most equal to .01 mhos/meter is negligible. When the conductivity is increased to .1 mhos/meter the error is approximately 16%.

SECTION IV

MONOCYCLE PULSE ANALYSIS

4.1 Introduction

A computer model is developed to predict the optimum radar parameters for a monocycle radar that detects a salt water wedge under fresh water and that can be used in bathymetry. It is shown that the monocycle that is reflected from a salt water wedge has a different shape than a monocycle that is reflected from a sandy bottom. If the velocity of propagation is known in the fresh water the depth to the salt water wedge or sandy bottom can be determined.

The model is then generalized to include m layers so that other cases of interest to the Navy can be analyzed. For example, a thermocline in the fresh water layer requires a four layer model. A mine buried in sand under fresh water that has a thermocline requires a five layer model.

The ability to locate and identify salt water wedges may be important for Anti-Submarine Warfare (ASW) and mine warfare. Remote measurement of fresh water depths may be useful to the Navy in bathymetry.

As throughout the entire report, the MKS system of units is used in this section.

4.2 Computer Model

It is assumed that a uniform plane electromagnetic wave propagates from

a height z = L above the air/fresh water interface. The complex propagation constant of uniform plane waves in medium m is denoted by k_m:

$$k_m = \{j\omega\mu_m(\sigma_m + j\omega\epsilon_m)\}^{1/2}$$

$$= \beta_m - j\alpha_m \qquad (18)$$

where

ω = $2\pi f$, angular frequency, radians/sec

f = frequency, Hertz

μ_m = magnetic permeability of medium m, Henry/meter

σ_m = conductivity of medium m, mhos/meter

ϵ_m = dielectric constant of medium m, Farad/meter

j = $\sqrt{-1}$, denotes the imaginary part of a complex number

The real part of the complex propagation constant, α_m, causes attenuation as the wave propagates. The imaginary part of the complex propagation constant, β_m, causes a phase shift in the wave as it propagates. In general, the real and imaginary part of the propagation constant are not perpendicular to each other. This gives rise to the concept of reactive power flow. Dropping the subscript m for the moment for convenience the real and imaginary parts of the complex propagation constant are:

$$\beta = \omega\sqrt{\epsilon\mu}\{1/2\{\sqrt{1+(\sigma/\omega\epsilon)^2}+1\}\}^{1/2} \qquad (19)$$

and

$$\alpha = \omega\sqrt{\varepsilon\mu}\{1/2\{\sqrt{1+(\sigma/\omega\varepsilon)^2}-1\}\}^{1/2} \qquad (20)$$

From equations (19) and (20) it is seen that the complex propagation constant is a function of two parameters: [25]

(a) $\omega\sqrt{\varepsilon\mu}$, which is the propagation constant of a uniform plane wave with $\sigma = o$, and

(b) $\sigma/\omega\varepsilon$, which is the loss tangent of the medium. It is the ratio of the conduction current, σE, to the displacement current $j\omega\varepsilon E$, in the dissipative medium.

The units of α, β and hence k are $(\text{meter})^{-1}$.

The reference, $z = 0$, it taken at the air/fresh water interface. The transmitter and receiver are at height $z = L$. The distance below the interface is negative and the salt water layer occurs at $z = -d$ meters. The salt water layer is considered to be infinite in depth.

The incident uniform electromagnetic plane wave in air is denoted by E_{t1}, H_{t1}, where the time harmonic dependence, $\exp(jwt)$, is understood.

$$E_{t1} = E_{to} \exp(-jk_1 z) \qquad (21)$$

and

$$H_{t1} = H_{to} \exp(-jk_1 z) \qquad (22)$$

The ratio of the amplitudes of equations (21) to (22) results in what is called the characteristic wave impedance or intrinsic impedance of the medium.[26] For this report the ratio will be referred to as the characteristic wave impedance of a uniform plane wave, or more succinctly the characteristic impedance. Its units are Ohms and it is defined by:

$$\eta_m = j\omega\mu_m/k_m \tag{23}$$

where

η_m = the characteristic impedance of layer m, Ohms

Taking the ratio of equations (22) to (21) and substituting equation (23), the incident magnetic field is expressed in terms of the incident electric field as:

$$H_{to} = 1/\eta_1 E_{to} \tag{24}$$

where

η_1 = the characteristic impedance of free space = 377 Ohms

Since the magnetic field intensity vector is obtained by dividing the electric field intensity vector by the characteristic impedance, only the electric field intensity vector will be given. Depending on the direction of the flow of energy and the mutual positions of the electric field intensity vector and the magnetic field intensity vector a sign change may also

take place. A normalized characteristic impedance is defined as the ratio of the characteristic impedance of layer m divided by the characteristic impedance of layer (m+1):

$$\eta_{m(m+1)} = \eta_m / \eta_{m+1} = \mu_m k_{m+1} / \mu_{m+1} k_m \tag{25}$$

By analogy with transmission line theory, it is possible to define a reflection coefficient as a function of the characteristic impedances. The reflection coefficient at the interface between layer m and m+1 is defined as

$$\Gamma_{m(m+1)} = (1-\eta_{m(m+1)})/(1+\eta_{m(m+1)}) \tag{26}$$

For non magnetic media

$$\mu_1 = \mu_2 = \cdots = \mu_m = \mu_o \tag{27}$$

where

μ_o = the magnetic permeability of free space, Henry/meter

Substituting equations (23) and (27) into (26) we have

$$\Gamma_{m(m+1)} = (k_m - k_{m+1})/(k_m + k_{m+1}) \tag{28}$$

For the case of a three layer system with distinct parallel boundaries,

medium 1 is air, medium 2 is fresh water and medium 3 is salt water. Figure 7 denotes the notation used in the model.

The incident electric field intensity vector is given by equation (21). The electric field reflected from the air/fresh water interface is denoted by:

$$E_{r1} = E_1 \exp(+jk_1 z) \tag{29}$$

Where E_1 is the amplitude of E_{r1} at $z = o$ and is related to the reflection coefficient between the air/fresh water interface. The electric field propagating in the fresh water is given by:

$$E_{t2} = E_2 \exp(-jk_2 z) \tag{30}$$

Where E_2 is the amplitude of E_{t2} at $z = o$ and is related to one plus the reflection coefficient between the air/fresh water interface. The electric field reflected from the fresh water/salt water interface is given by:

$$E_{r2} = E_2' \exp(+jk_2 z) \tag{31}$$

Where E_2' is the amplitude of E_{r2} at $z = -d$ and is related to the reflection coefficient between the fresh water/salt water interface. The wave propagating in the salt water is given by:

$$E_{t3} = E_3 \exp(-jk_3 z) \tag{32}$$

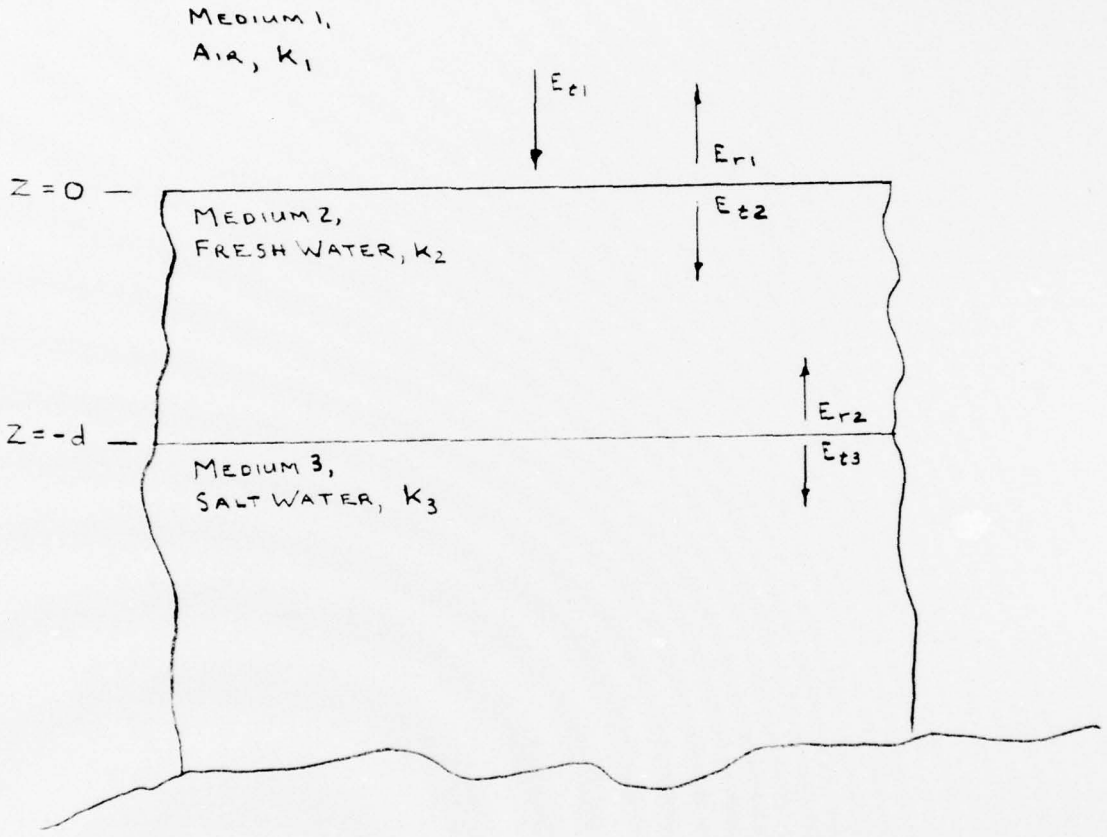

Note: The arrows denote the directions of propagation. The electric field vectors are parallel to the boundaries.

Figure 7. A model for 3 media.

where E_3 is the amplitude of E_{t3} immediately after it is transmitted into the salt water.

It can be shown by using equations (21) through (28) that the overall reflection coefficient in air of the three layered system is

$$\Gamma(\omega) = \{\Gamma_{12}+\Gamma_{23}\exp(-j2k_2d)\}/\{1+\Gamma_{12}\Gamma_{23}\exp(-2jk_2d)\} \quad (33)$$

where

d = the depth of the fresh water, meters

Γ_{12} = the reflection coefficient at the air/fresh water interface

Γ_{23} = the reflection coefficient of the fresh water/salt water interface

From equation (28) it is seen that

$$\Gamma_{12} = (k_1-k_2)/(k_1+k_2) \quad (34)$$

$$\Gamma_{23} = (k_2-k_3)/(k_2+k_3) \quad (35)$$

If it is assumed that a pulse of form $e_t(t)$ is emitted at a height $z = L$ above the air/fresh water interface, and that $E_t(\omega)$ is the Fourier transform of $e_t(t)$, then $E_{to}(\omega)$ is given by:

$$E_{to}(\omega) = E_t(\omega)\exp(-jk_1L) \quad (36)$$

and at z = o the electric field reflected from salt water wedge can be written as:

$$E_r(\omega) = E_t(\omega)\Gamma(\omega)\ \exp(-jk_1 L) \tag{37}$$

The reflected pulse, in the time domain, at any height z in the air above the fresh water interface is given by

$$e_r(z,t) = (1/2\pi)\int_{-\infty}^{+\infty} E_t(\omega)\Gamma(\omega)\ \exp\{-j(k_1 L + k_1 z - \omega t)\}d\omega \tag{38}$$

where the inverse Fourier transform was taken of equation (37) and the delay factor $\exp(-jk_1 z)$ has been added. Suppose that the pulse has a narrow spectrum, where narrow is defined as ± 10% of the center frequency of the monocycle pulse, and that over the band Γ_{12} and Γ_{23} can be regarded as constant. Then the reflected pulse is written

$$e_r(z,t) = (1/2\pi)\int_{\omega o-\Delta\omega/2}^{\omega o+\Delta\omega/2} E_t(\omega)\{\{\Gamma_{12}+\Gamma_{23}\ \exp(-j2k_2 d)\}/$$

$$\{1-\Gamma_{21}\Gamma_{23}\exp(-j2k_2 d)\}\}\exp j\omega\{t-(z+L)/C_1\}d\omega \tag{39}$$

where

$$\Gamma_{21} = -\Gamma_{12} \tag{40}$$

and

c_1 = the velocity of electromagnetic energy in air, meters/sec

To account for multiple reflection of the single frequency waves that comprise the monocycle pulse within the fresh water layer, the reflection coefficient is written as:

$$\Gamma(\omega) = (\Gamma_{12}+\Gamma_{23}\exp(-2jk_2d))/(1-\Gamma_{21}\Gamma_{23}\exp(-j2k_2d))$$

$$= \Gamma_{12}+\Gamma_{23}\exp(-2jk_2d)\Sigma_{m=o}^{\infty}(\Gamma_{21}\Gamma_{23}\exp(-2jk_2d))^m$$

$$= \Gamma_{12}+\Sigma_{m=1}^{\infty}(\exp(-j2mk_2d))(1+\Gamma_{12})\Gamma_{23}(1+\Gamma_{21})(\Gamma_{21}\Gamma_{23}) \qquad (41)$$

The terms can now be interpreted. The term Γ_{12} is the reflection coefficient from the air/fresh water interface. The factor $(1-\Gamma_{12})$ is the transmission coefficient at the air/fresh water interface. The factor Γ_{23} is the reflection coefficient at the fresh water/salt water interface, and the factor $1+\Gamma_{21}$ is the transmission coefficient at the fresh water/air interface. The factor $\exp(-2jk_2d)$ accounts for the attenuation and phase delay of a wave travelling back and forth one time in the fresh water layer. Hence, the combination of terms $\exp(-2jk_2d)(1+\Gamma_{12})\Gamma_{23}(1+\Gamma_{21})$ is the net reflection coefficient of a wave passing through the air/fresh water interface, reflecting from the fresh water/salt water interface and passing through the fresh water/air interface. Successive terms in the series multiply this combination by $\exp(-2jk_2d)\Gamma_{12}\Gamma_{23}$. This represents single frequency waves which

have undergone multiple reflection within the fresh water layer before passing out through the fresh water/air interface. Although mathematically the single frequency waves are represented as undergoing multiple reflections, it is shown in Section 4.3 that a clearly defined monocycle pulse is reflected from each interface.

Substituting equation (41) into equation (39), we have,

$$e_r(z,t) = (1/2\pi)\int_{\omega o-\Delta\omega/2}^{\omega o+\Delta\omega/2} E_t(\omega)(\Gamma_{12}+\Sigma_{m=1}^{\infty}(\exp(-2mjk_2d))(1+\Gamma_{12})\Gamma_{23}(1+\Gamma_{21})$$

$$(\Gamma_{21}\Gamma_{23})^{m-1}\exp j\omega(t-(z+L)/c_1))d\omega \qquad (42)$$

Let

$$k_2 = \beta_2 - j\alpha_2 \qquad (43)$$

Then

$$\exp(-2mjk_2d) = \exp(-2m\alpha_2 d)\ \exp(-2jm\beta_2 d) \qquad (44)$$

Also let

$$\beta_2 = \omega/c_2 \qquad (45)$$

where

c_2 = the velocity of propagation of electromagnetic energy in fresh water, meters/sec

Then the reflected pulse is given by

$$e_r(z,t) = (1/2\pi)\Gamma_{12}\int_{\omega o-\Delta\omega/2}^{\omega o+\Delta\omega/2} E_t(\omega)\ \exp j\omega(t-(z+L)/c_1)\,d\omega$$

$$+(1+\Gamma_{12})\Gamma_{23}(1+\Gamma_{21})\Sigma_{m=1}^{\infty}(\Gamma_{21}\Gamma_{23})^{m-1}(1/2\pi)$$

$$X\int_{\omega o-\Delta\omega/2}^{\omega o+\Delta\omega/2} E_t(\omega)\exp(-2m\alpha d)(\exp j\omega(t-(z+L)/c_1-2md/c_2)\,d\omega \qquad (46)$$

If the attenuation can be regarded as frequency independent over the frequency band of the pulse, then we see that the incident pulse gives rise to a succession of reflected pulses of the same shape as the incident pulse but phase shifted, reduced in magnitude and delayed in time be the amount $(z+L)/c_1+2md/c_2$. This result is significant because it shows that, a narrow band pulse is not changed in shape by the interface it is reflected from. It is shown in Section 4.3 that a broadband monocycle pulse is changed in shape by the different layers from which it is reflected.

4.3 Broadband Monocycle Pulse

A broadband monocycle pulse is computer programmed to show that it is possible to distinguish a salt water wedge from a sandy bottom. The pulse reflected from the air/fresh water interface first appears on an A scope. From its time of arrival the pilot knows how high he is above the fresh water. The next pulse to appear on the scope is either the one reflected from the salt water wedge or the sandy bottom. It is shown that these two pulses differ drastically in shape and, hence, one can identify whether the monocycle has been reflected from salt water or a sandy bottom. By approx-

imating the velocity of propagation in the fresh water layer the depth of the salt water wedge and sandy bottom can also be determined.

The incident pulse is of the form

$$e_t(t) = \begin{cases} A\sin^2(\pi t/\tau), & o<t>\tau \quad (47) \\ o \quad , & t<o, t>\tau \quad (48) \end{cases}$$

The magnitude of the normalized pulse in Volts/meter is plotted in Figure 8. The width of the pulse at its base is 10 ns. It can be shown that the Fourier transform of the incident pulse is

$$E_t(\omega) = \int_{-\infty}^{+\infty} e_t(t) e^{-j\omega t} dt$$

$$= -A(2\pi/\tau)^2 \exp(-j\omega\tau/2)\{\sin(\omega\tau/2\}/$$

$$\omega\{\omega^2-(2\pi/\tau)^2\} \quad (49)$$

The power spectrum of the reflected pulse is given by:

$$P_r(\omega) = |E_t(\omega)|^2 |\Gamma(\omega)|^2 \quad (50)$$

Where $E_t(\omega)$ is given by equation (49) and $\Gamma(\omega)$ is given by equation (41). The reflected pulse is

$$e_r(t) = 1/2\pi \int_{-\infty}^{+\infty} E_t(\omega)\Gamma(\omega) e^{j\omega t} d\omega \quad (51)$$

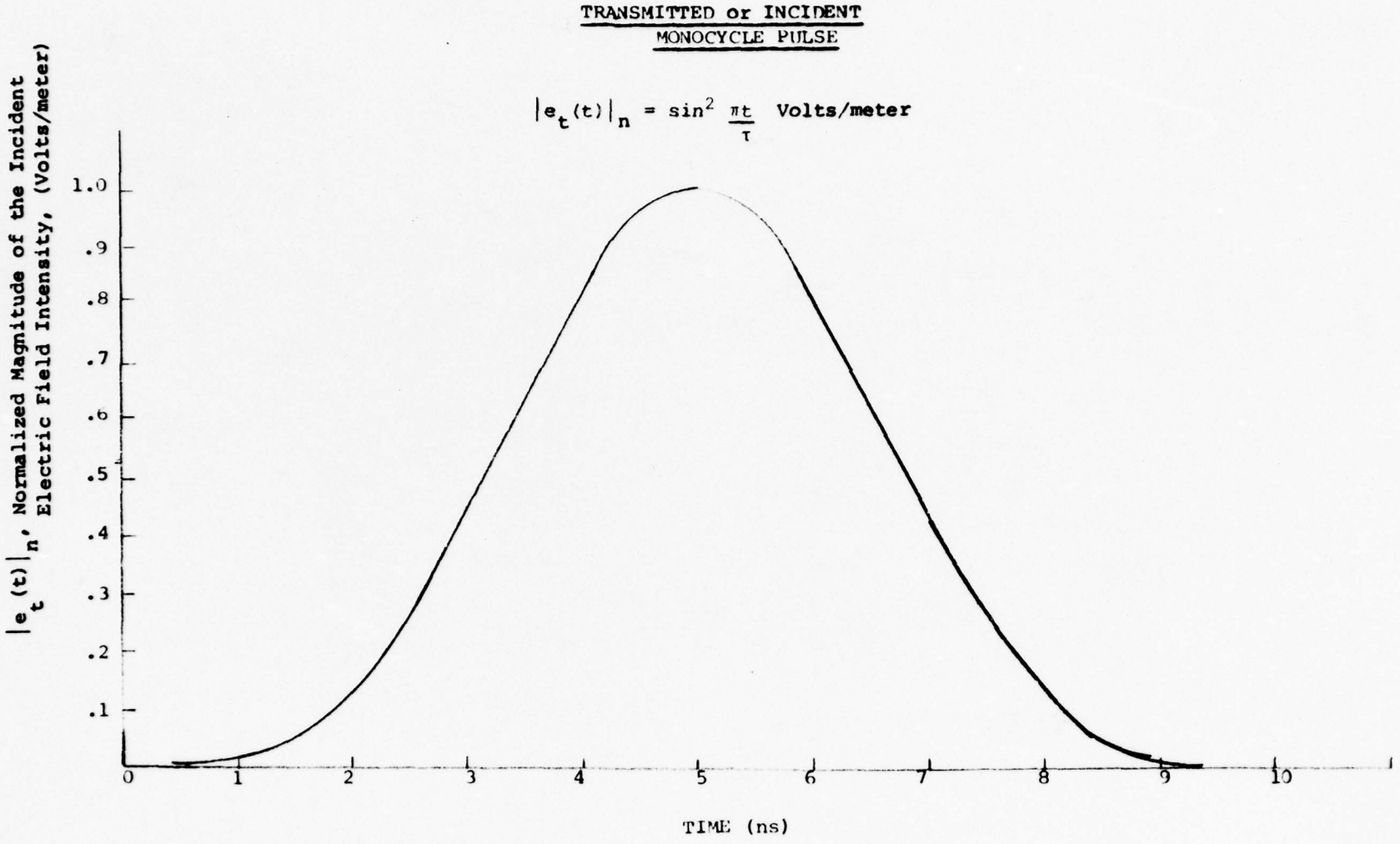

Figure 8. Transmitted Monocycle Pulse vs. Time.

To utilize equation (51) in the computer model, it is written as a discrete Fourier transform:

$$e_t(K\Delta t) = (\Delta f/2F_{max}) \sum_{n=-N/2}^{N/2} E_t(\omega_n)\Gamma(\omega_n)\exp(j2\pi nk\Delta t/\tau_{max})$$

$$k = 0,1,\cdots,N-1 \qquad (52)$$

where

ω_n = $2\pi n\Delta f$, angular frequency, radians

F_{max} = $(N/2)\Delta f$, units Hertz

τ_{max} = $N\Delta t$, ns

In using the Fast Fourier Transform (FFT) to evaluate equation (52), after Nyquist,[27] N is chosen to be a power of 2 large enough so that the sampling rate is at least twice as high as the largest significant frequency in the power spectrum in order to avoid the aliasing problem.[28]

Equation (52) is computer programmed and the results of transmitting pulses through different materials is analyzed by its evaluation. The computer model represents three layers. They are air, fresh water and salt water. For a comparison of pulses reflected from different materials, the salt water layer is changed to wet sand. The constitutive parameters of wet sand are approximated to be $\varepsilon = 30$ and $\sigma = .03$ mhos/meter.[29] The transmitted pulse, shown in Figure 8 is reflected from the air/fresh water interface. Figure 9 is a plot of the reflected pulse. The maximum amplitude of the pulse is .79 Volts/meter for a normalized incident amplitude of 1 Volt/meter. Its

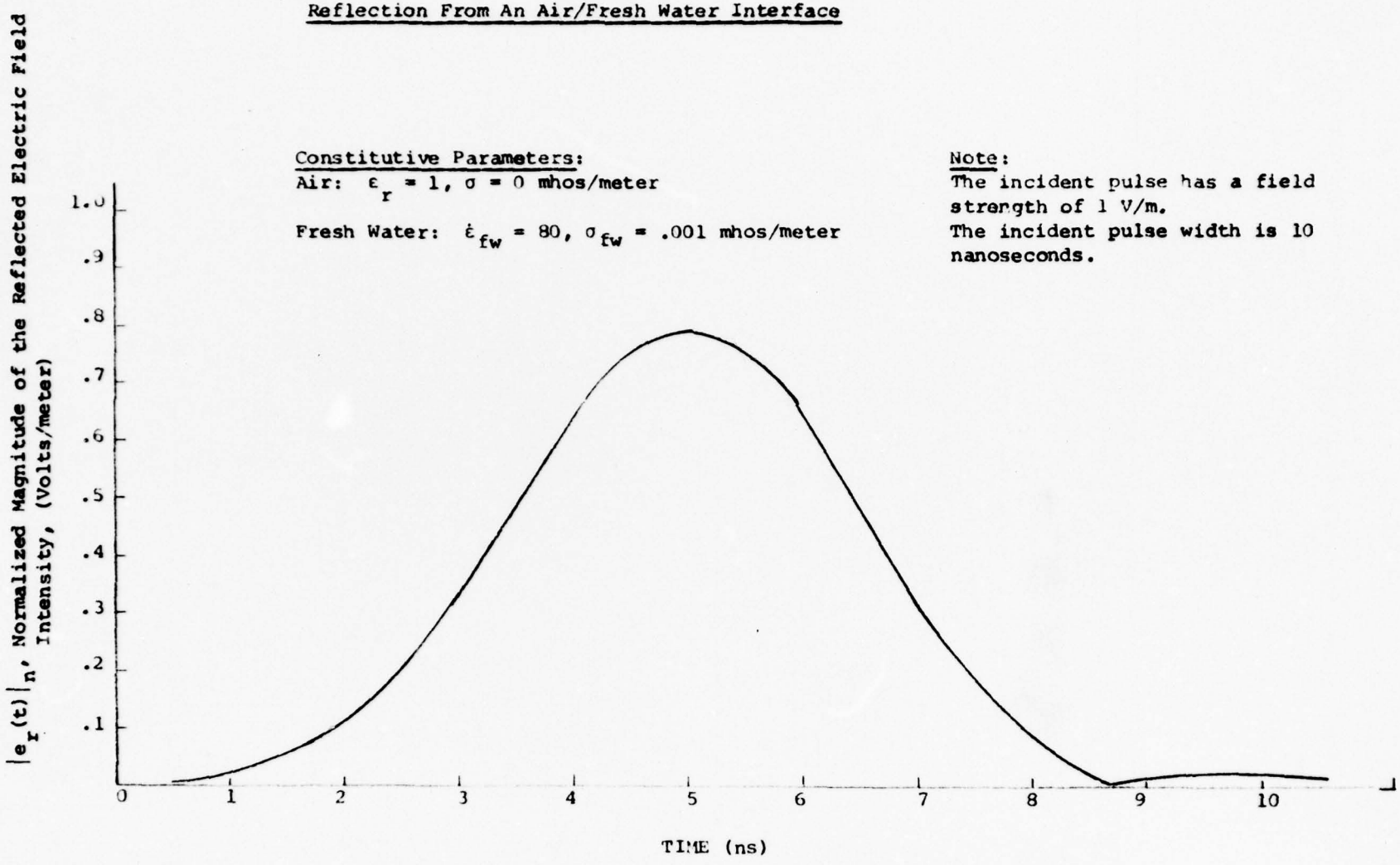

Figure 9. Monocycle pulse reflected from an air/fresh water interface vs. time.

width is equal to the width of the transmitted pulse. This is to be expected since air is not a dispersive medium. It has a slight undershoot not present in the transmitted pulse. This undershoot is significant because it identifies the pulse as reflected from fresh water.

The pulse then propagates through the fresh water and is reflected from the fresh water/salt water interface or the fresh water/wet sand interface. Figure 10 is a plot of the pulse reflected from a salt water wedge. It has an amplitude of .22 Volts and a 6 dB width of 4 ns compared to 1 Volt and 3.5 ns for the incident pulse. The pulse seems raised as if on a pedestal with the leading edge approaching zero faster than the trailing edge. The base of the pulse is approximately 3 times greater than that of the transmitted pulse. There is no difficulty in identifying which pulse is reflected from fresh water and which one is reflected from salt water. It now remains to be proven by experimentation. A further computer search in which common materials such as mud, and other types of bottoms might also be a useful excercise.

In the model the depth of the fresh water is 5 meters. The peak of the reflected pulse occurs at 303.6 ns. Scaling the velocity of propagation by the square root of the dielectric constant and dividing by two gives the time the pulse is reflected from the salt water wedge. The difference between the calculated time and the time obtained from the computer model is .31 ns, a 1.9% error.

Figure 11 is a plot of the pulse reflected from wet sand. It has an

Reflection From A Fresh Water/Salt Water Interface

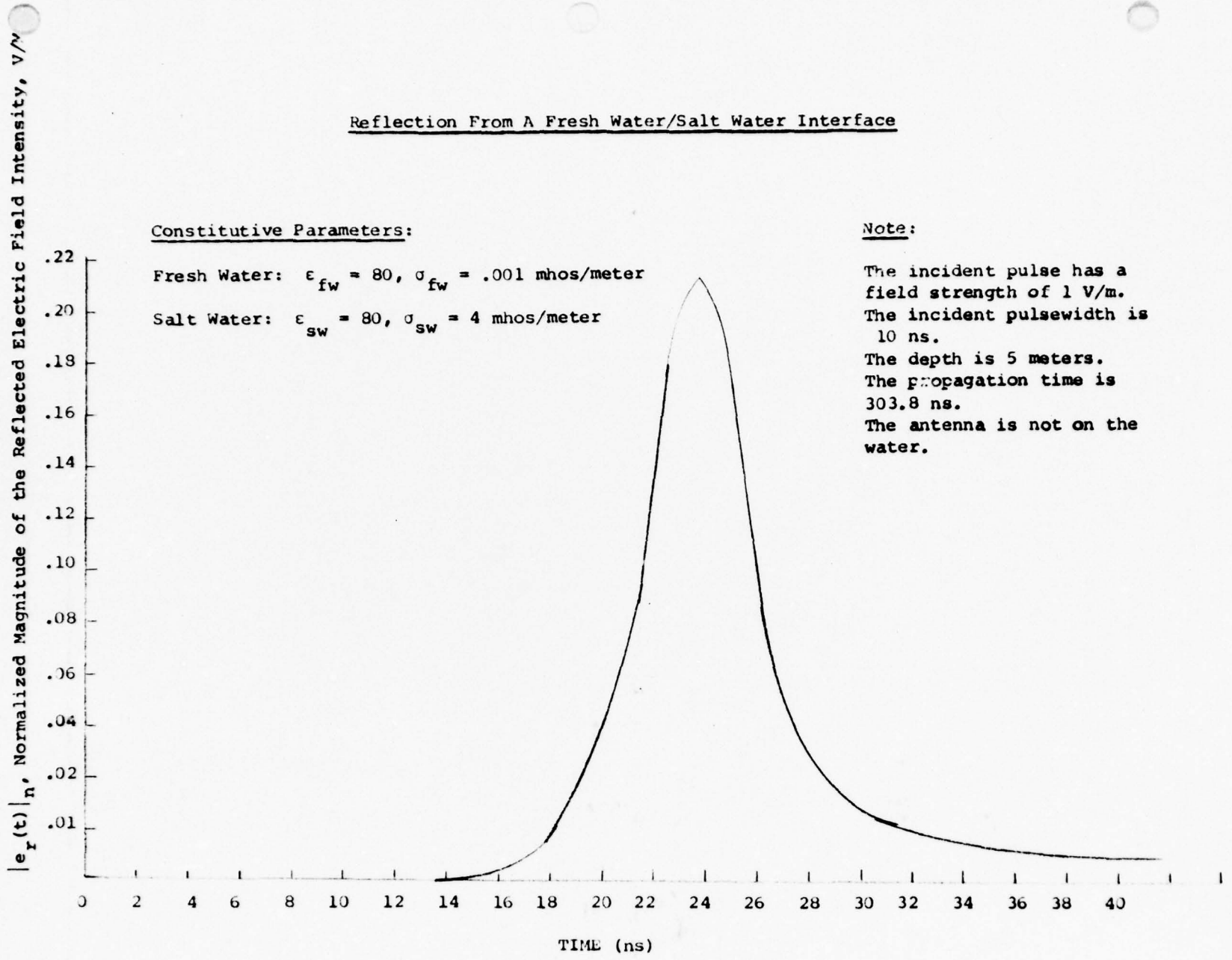

Figure 10. Monocycle pulse reflected from a salt water/fresh water interface vs. time.

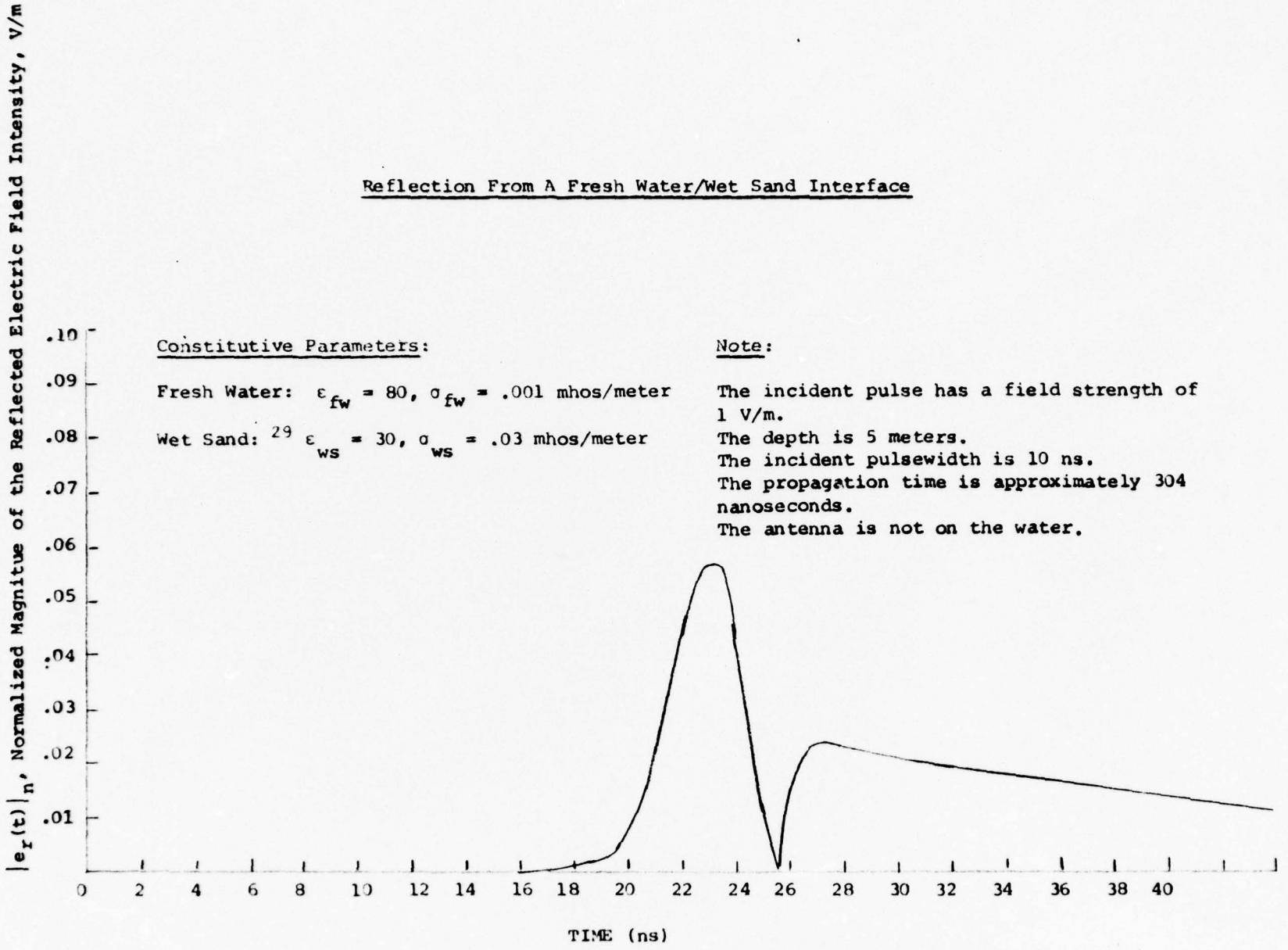

Figure 11. Monocycle pulse reflected from a fresh water/wet sand interface vs. time.

amplitude of .057 Volts with an undershoot that has an amplitude of .024 Volts. The "main lobe" has a 6 dB width of 3 ns but the base of the pulse is spread out approximately 4 times greater than the transmitted pulse. The large difference between the pulse shapes show it is feasible to determine what the second layer is by examining the return pulse. This is provided there are no reflections from nearby targets (within depth range) to clutter the main interface return as may occur near structures and breakwaters.

The computer program was modified so that it graphically presents the data. In the computer model, it is assumed that a plane wave is incident on the boundaries, (i.e. the monocycle radar antenna is at infinity), and that the incident pulse has field strength of 1 Volt/meter. The depth of the fresh water layer is 5 meters and the pulsewidth is 10 ns. The computer plot in Figure 12 presents the pulse reflected from the air/fresh water interface. As expected its amplitude is .79 Volt/meter. The fresh water/sand interface is presented in the same graph. Its amplitude is .06 Volt/meter. The propagation time is approximately 304 ns. The constitutive parameters of the fresh water are: $\varepsilon_{fw} = 80$, $\sigma_{fw} = .001$ mhos/meter. The constitutive parameters of the salt water are kept constant throughout the computer runs and are: $\varepsilon_{sw} = 80$, $\sigma_{sw} = 4$ mhos/meter. The computer plot for a monocycle pulse reflected from salt water is presented in Figure 13. The pulse reflected from the air/fresh water interface is .79 Volt/meter. The pulse reflected from the fresh water/salt water interface has an amplitude of .23 Volt/meter. The time of propagation is 304 ns. Although the computer plot is "rough", the marked difference between the return pulse from wet sand compared to the pulse returned from salt water is still apparent.

Figure 12. Monocycle pulse reflected from an air/fresh water interface and a fresh water/wet sand interface vs. time.

Figure 13. Monocycle pulse reflected from an air/fresh water interface and a fresh water/salt water interface vs. time.

The computer model was then modified so that the antenna is on the water. A 100 ns pulse is transmitted and it is assumed that it is 1 Volt/meter at the surface of the water. The depth to the salt water layer is, as before, 5 meters. The data used for the constitutive parameters is for the West Gotland Basin. The salinity varies with temperature in the basin and four values were used. Figure 14 shows that the pulse reflected from the salt water has an amplitude of .4 mV/meter. The conductivity is .8 mhos/meter or the salinity in the West Gotland Basin is 7.5 ppt for a temperature of T = 5°C. When the temperature in the basin increases to 10°C for a salinity of 75 ppt, the conductivity is .92 mhos/meter. The amplitude of the pulse reflected from the salt water is .35 mV/meter (See Figure 15). For T = 5°C and a salinity of 10 ppt in the basin, the conductivity is 1.06 mhos/meter. The amplitude of the pulse reflected from the salt water is .32 mV/meter (See Figure 16). Increasing the temperature to T = 10°C for a salinity of 10 ppt results in a conductivity of 1.2 mhos/meter. Figure 17 shows that the pulse reflected from the salt water wedge has an amplitude of .28 mV/meter. All of the results for the West Gotland Basin are for a 1 Volt/meter, 100 ns pulse that is transmitted from an antenna on the surface of the "fresh water". The pulse propagates through 5 meters of water in the basin, is reflected from a salt water wedge and returns to the antenna.

The increase in conductivity delayed the return of the pulse. For example, when the conductivity is .001 mhos/meter, the total propagation time is 304 ns. Increasing the conductivity to .8 mhos/meter, increased the propagation time to 16 μs. The propagation time is increased by a factor of 53. Increasing the conductivity to 1.06 mhos/meter, increased the propagation time to 20 μs, a

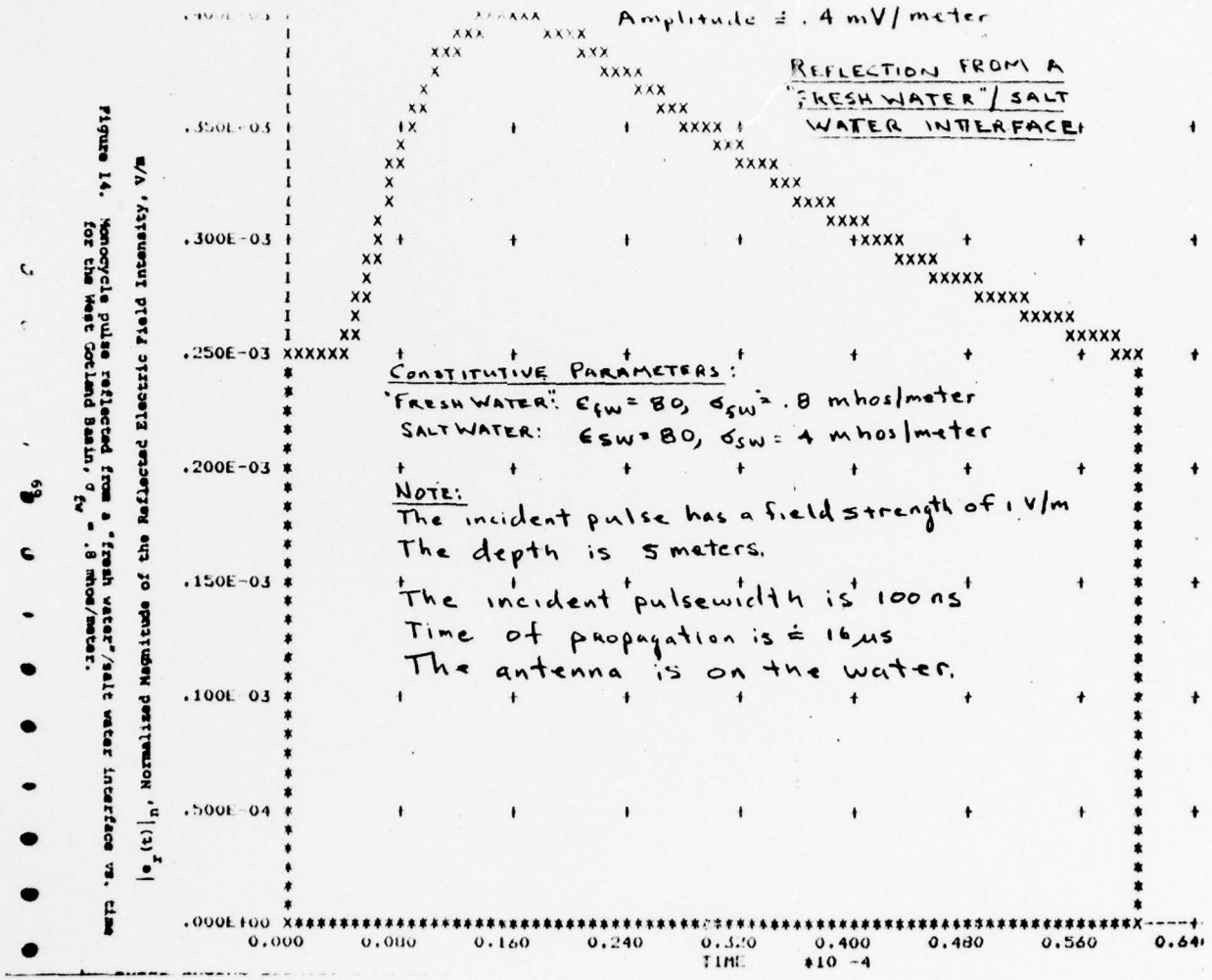

Figure 14. Monocycle pulse reflected from a "fresh water"/salt water interface vs. time for the West Gotland Basin, $\sigma_{fw} = .8$ mhos/meter.

$|e_r(t)|_n$, Normalized Magnitude of the Reflected Electric Field Intensity, V/m

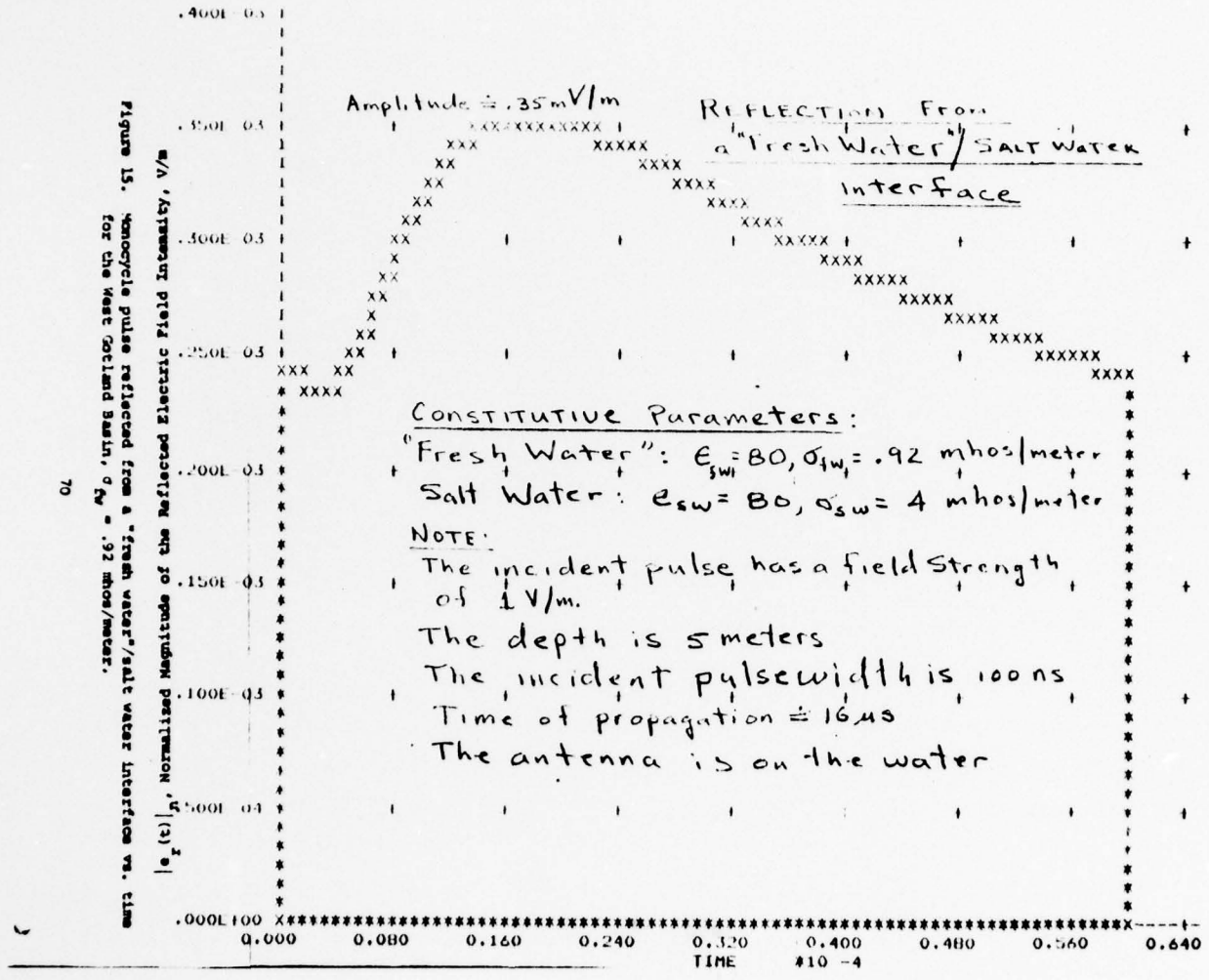

Figure 15. Monocycle pulse reflected from a "fresh water"/salt water interface vs. time for the West Coast Sea, σ_{fw_1} = .92 mhos/meter.

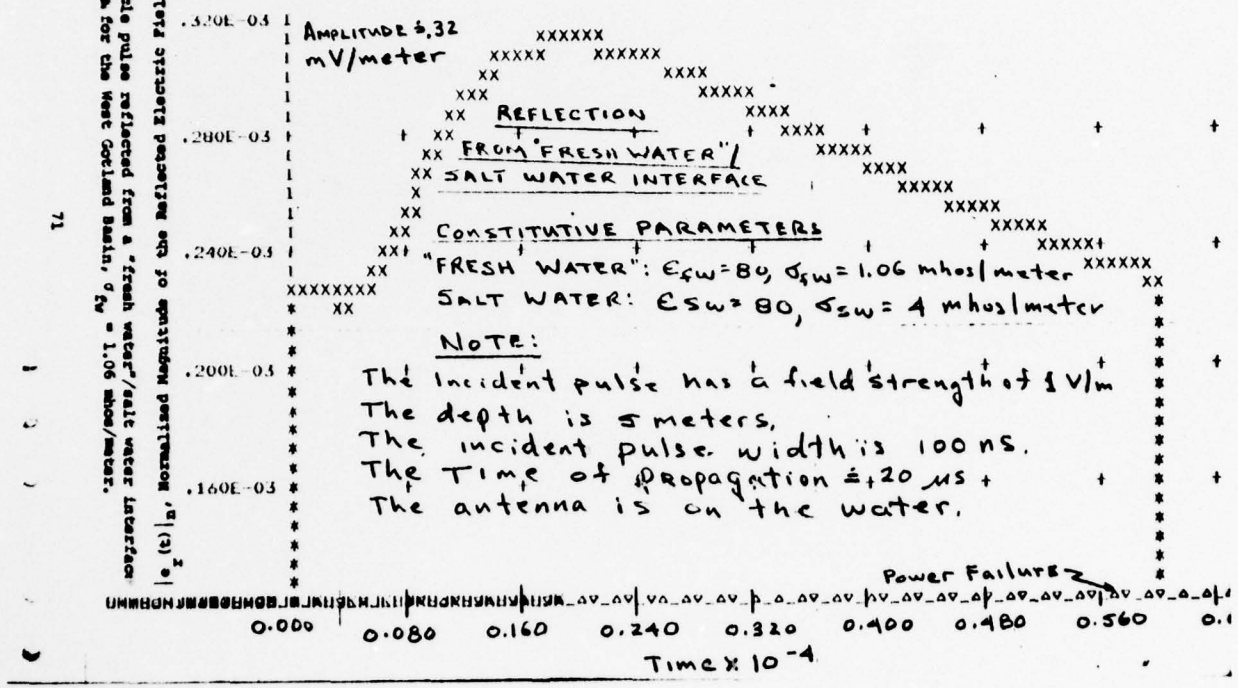

Figure 16. Monocycle pulse reflected from a "fresh water"/salt water interface vs time for the West Gotland Basin, σ_{fw} = 1.06 mhos/meter.

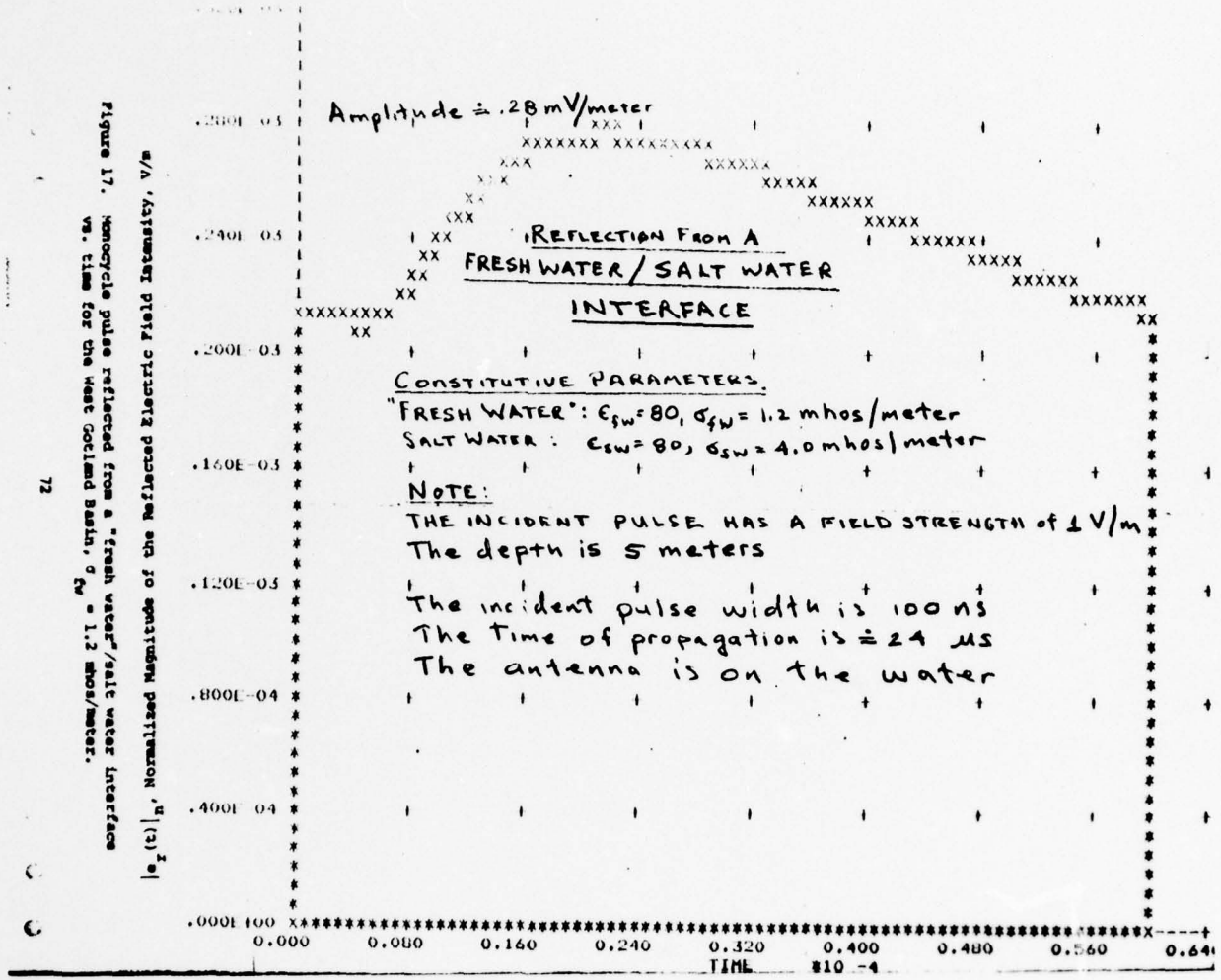

Figure 17. Monocycle pulse reflected from a "fresh water/salt water interface
vs. time for the Goetsch Test, σ_{fw} = 1.2 mhos/meter.

$|e_x(t)|_n$, Normalized Magnitude of the Reflected Electric Field Intensity, V/m

factor of 67 and an increase in conductivity to 1.2 mhos/meter increased the propagation time by 80.

The results are of great significance. First they show that the return from a salt water wedge in the West Gotland basin is of the order of Milli Volts/meter and second the delay due to the conductivity, which can be as high as a factor of 80 over air must be accounted for to properly range gate the signal. The reason for the increase in propagation time is the conductivity dominates the dielectric constant when computing the propagation constant, β.

4.4 A Generalized Computer Model For m+1 Layers

The general reflection coefficient for a system of m+1 parallel plane layers is developed to account for the thermocline which represents a fourth layer and in case two thermoclines or other possible variations such as an air/fresh water interface, thermocline, fresh water/sand interface and sand/mine interfaces are eventually evaluated. Figure 18 shows the notation used for a system of m+1 parallel plane layers.

The generalized overall reflection coefficient is written in a closed form expressed in continued fractions. The method is discussed shortly. The reflection coefficient is:

$$\Gamma(\omega) = 1/\Gamma_{12} + \{1-(1/\Gamma_{12}^{2})\}\exp(j2k_{2z}d_{2})//(1/\Gamma_{12})\exp(j2k_{2z}d_{2})$$

$$+ 1/\Gamma_{23} + 1-(1/\Gamma_{23}^{2})\exp(j2k_{3z}(d_{3}-d_{2}))//(1/\Gamma_{23})\exp(j2k_{3z}(d_{3}-d_{2}))$$

$$+ \cdots + 1/\Gamma_{(m-1)m} +$$

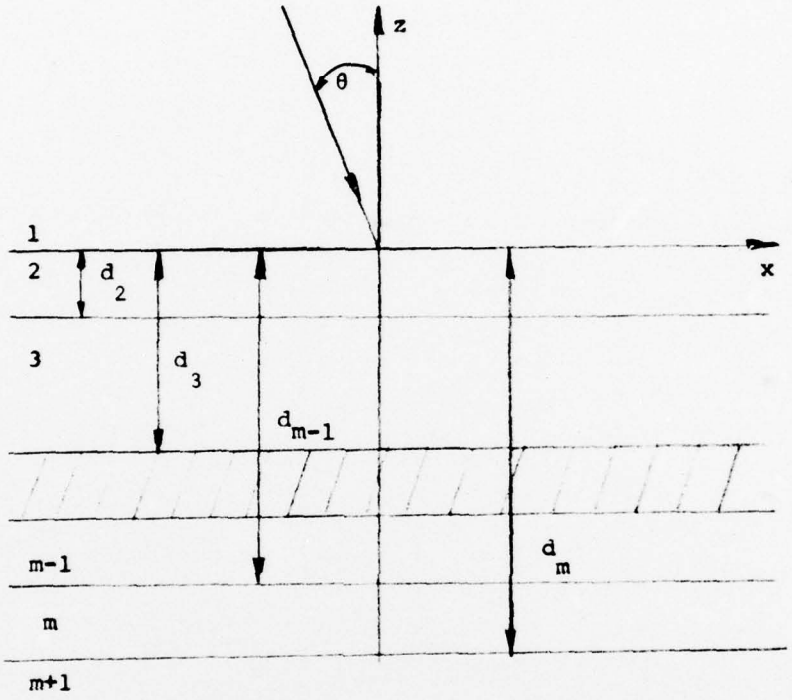

Figure 18. A system of m+1 parallel plane layers

$$+ 1-(1/\Gamma^2_{(m-1)m})\}\exp\{j2k_{mz}(d_m-d_{m-1})\}//(1/\Gamma_{(m-1)m})\exp\, j2k_{mz}(d_m-d_{m-1})\}$$

$$+\Gamma_{m(m+1)} \tag{53}$$

where

$$k_\ell^2 = k_x^2+k_{\ell z}^2 = \omega^2\mu\varepsilon_\ell, \quad \ell = 1,2,\cdots,m+1 \tag{54}$$

$$k_x = k_1 \sin\theta, \tag{55}$$

and

$$\Gamma_{\ell(\ell+1)} = \begin{cases} (1-d_{(\ell+1)z}/k_{\ell z})/(1+k_{(\ell+1)z}/k_{\ell z}), \text{ TE waves} & (56) \\ \qquad\qquad\qquad\qquad\qquad\qquad \ell = 1,2,\cdots m \\ (1-\varepsilon_\ell k_{(\ell+1)z})/\varepsilon_{\ell+1} k_{\ell z}, \text{ TM waves} & (57) \end{cases}$$

The expression for the reflection coefficient given in equation (53) is a closed form solution expresses in continued fractions. The method is as follows: The reflection coefficient for any particular system is obtained from equation (53) by taking terms starting from the last one, until the subscript (m=1) of $\Gamma(m-1)m$ becomes equal to one. To clarify what is meant by the continued fraction notation, equation (53) is rewritten as

$$\Gamma = 1/\Gamma_{12}+N_{12}//D_{12}+1/\Gamma_{23}+N_{23}//D_{23}+\cdots+1/\Gamma_{(m-1)m}+N_{(m-1)}//D_{(m-1)m}$$
$$+\Gamma_{(m+1)m} \tag{58}$$

where

ω has been dropped from $\Gamma(\omega)$ for convenience in equations (58) through (63).

where

$$N_{(m-1)m} = (1-(1/\Gamma^2_{(m-1)m}) \exp j2k_{mz}(d_m - d_{m-1}), \tag{59}$$

$$D_{(m-1)m} = (1/\Gamma_{(m-1)m}) \exp j2k_{mz}(d_m - d_{m-1}). \tag{60}$$

For m=1 we have reflection from a half space, and

$$\Gamma = \Gamma_{12} \tag{61}$$

For m=2 we have one layer between two half spaces and

$$\Gamma = 1/\Gamma_{12} + N_{12}/(D_{12} + \Gamma_{23}) \tag{62}$$

For m=3 we have two layers between two half spaces and

$$\Gamma = 1/\Gamma_{12} + N_{12}/(D_{12} + \Gamma_{23}/(N_{23}/D_{23} + \Gamma_{34})). \tag{63}$$

The method can be continued for any number of layers. For a thermocline in a fresh water layer over a salt water wedge, equation (63) is substituted into equation (52).

4.5 Conclusion

It is feasible to detect and identify a salt water wedge using a broadband monocycle pulse. The analysis demonstrates that, if a narrow band pulse is used to detect a salt water wedge, the reflected pulse will be the same shape as the transmitted pulse. It is therefore not possible to identify what the pulse is

reflected from.

When a broadband pulse is transmitted it is possible to distinguish between the transmitted pulse and the pulses reflected from the air/fresh water and fresh water/salt water interfaces. It is also possible to tell if the salt water is not present and if the pulse is reflected from wet sand beneath the fresh water layer.

The pulse reflected from the air/fresh water interface is similar in shape to the transmitted pulse except for an undershoot. The pulse reflected from the salt water interface is different from the transmitted pulse. Its base width is elongated at least 3 pulse widths. A pulse reflected from wet sand has a negative undershoot not present in the pulse reflected from salt water.

The computer model, modified to simulate the temperatures and salinities of the West Gotland Basin showed that, for a 100 ns pulse propagating through 5 meters of water with conductivities of 1.2 mhos/meter, .28 mV/meter returned to a monocycle radar antenna on the surface of the water. The model also showed that when the conduction current dominates the displacement current delays in propagation as high as 80 can be expected.

These results are significant because they show that this method is applicable to detection and identification of salt water wedges beneath fresh surface waters. They also present a rapid remote method for use in bathymetry.

SECTION V

TYPICAL MONOCYCLE RADAR DESIGN PARAMETERS

5.1 Introduction

The preceeding analysis of electromagnetic energy propagating through and reflecting from dissipative media has led to the following typical desing of an airborne monocycle radar for use near-shore in bathymetry and detection and identification of salt water wedges.

5.2 Antennas

Figure 19 is a block diagram depicting the various components on a systems level of the monocycle radar. It consists of a transmit/receive antenna that is in general a broadband loaded dipole or travelling wave antenna. Several configurations are presented in Figure 20. They are travelling wave antennas, and a loaded dipole. The termination on the travelling wave antenna shown in Figure 20a absorbs reflections from the monocycle pulse reducing ringing To the input it seems as though the energy travels down a semi-infinite line. The travelling wave antenna is, by nature of its construction, suited for monocycle transmission. Monocycle operation can be improved somewhat by using the travelling wave antenna shown in Figure 20b. Widening the elements improve the impedance match over the bandwidth of the monocycle. Typical radiation patterns for a single frequency travelling wave antenna similar to the one shown in Figure 20a are shown in Figure 21.[30] The monocycle patterns are broader but have the same general shape. The patterns for a travelling wave antenna are tilted forward and have higher directivity than an equivalent length standing wave

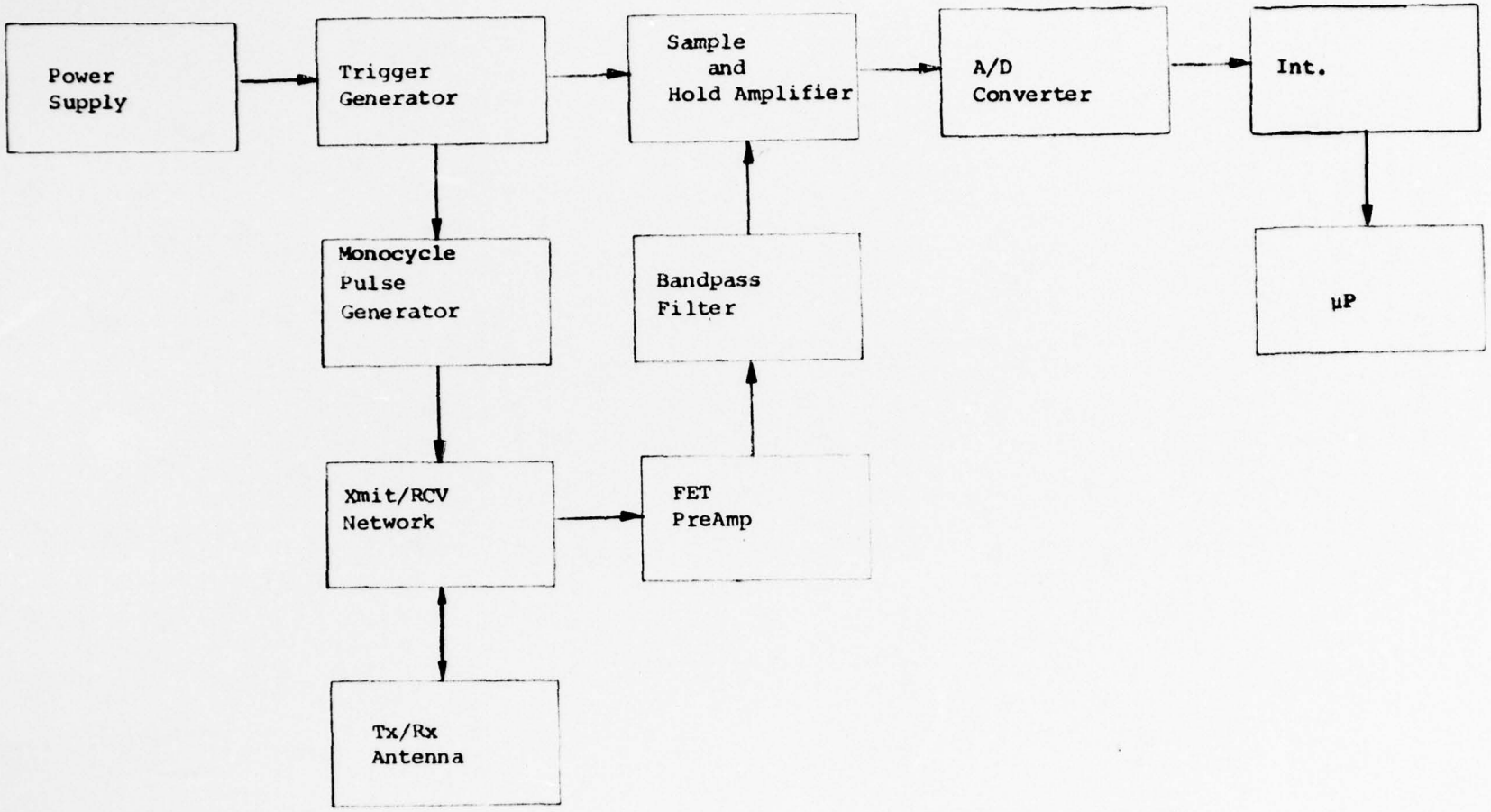

Figure 19. A block diagram of typical monocycle radar

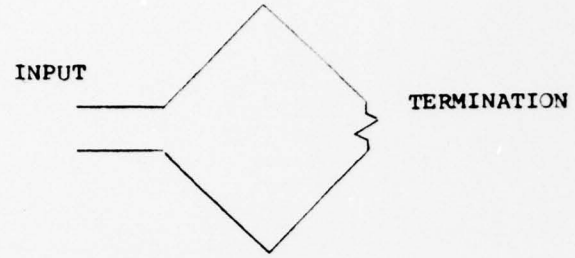

a. Travelling wave antenna

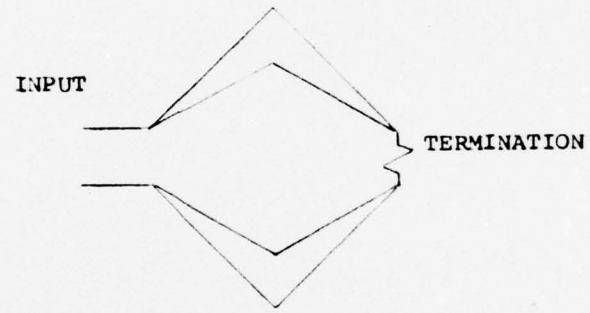

b. Travelling wave antenna modified for broadband application

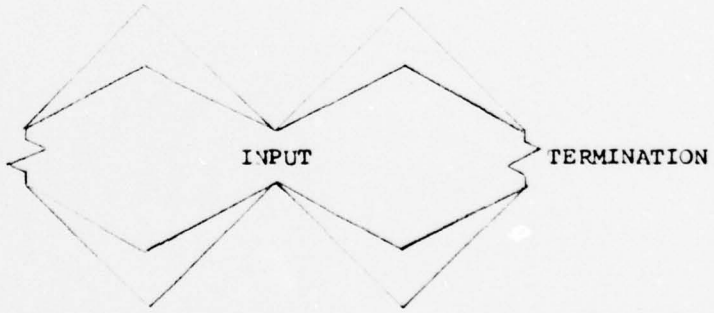

c. Broadband folded dipole

Figure 20. Antennas

AD-A076 621 BERTRAM ASSOCIATES MERRIMACK NH F/G 8/3
REMOTE IDENTIFICATION OF A SALT WATER WEDGE THROUGH DISSIPATIVE--ETC(U)
OCT 79 C L BERTRAM , R A SHORE N00014-79-C-0160
UNCLASSIFIED NL

2 OF 2
AD
A076621

END
DATE
FILMED
12-79
DDC

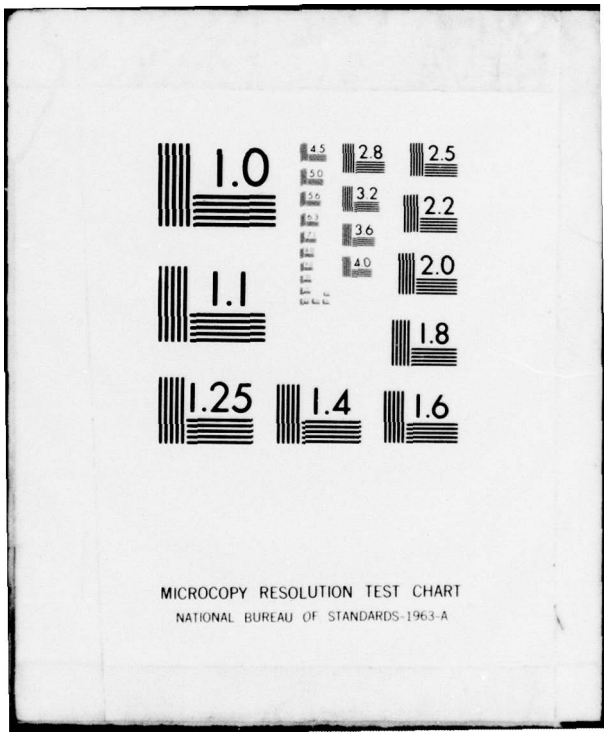
1.0
1.1
1.25
1.4
1.6
1.8
2.0
2.2
2.5
2.8
3.2
3.6
4.0
4.5
5.0
5.6
6.3
7.1
MICROCOPY RESOLUTION TEST CHART
NATIONAL BUREAU OF STANDARDS-1963-A

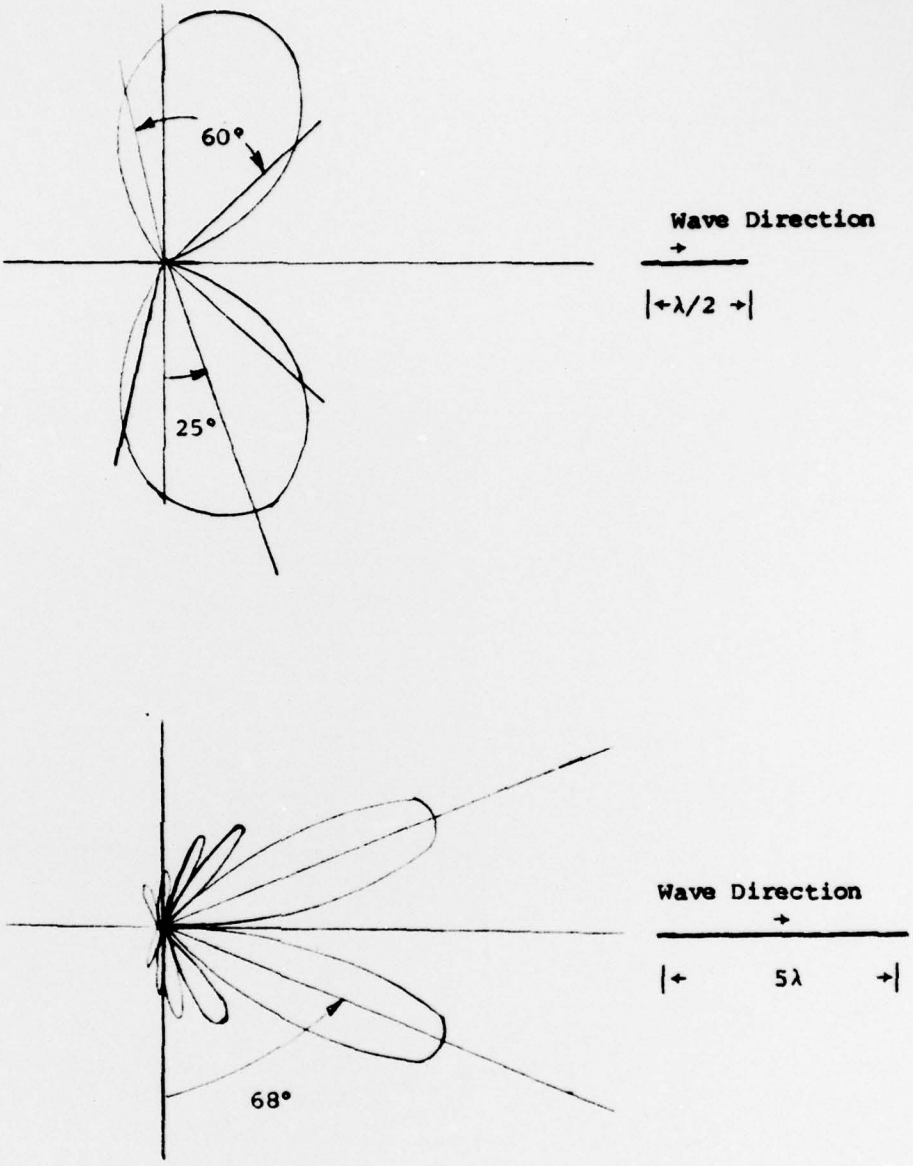

Note: The phase velocity along the antenna is equal to that of light.

Figure 21. Radiation patterns of a travelling wave antenna. [30]

antenna. A variation of the travelling wave antenna is shown in Figure 14c. It is essentially a broadband folded dipole. The radiation pattern of this antenna does not "squint" like the travelling wave antenna.

If the conductivity of the fresh water layer is less than, at most equal to, .01 mhos/meter, the width of the monocycle pulse can be of the order of a nanosecond. For this case, it is more efficient to radiate a single lobe and direct to radiate all of the energy towards the target. The TEM antenna[31] shown in Figure 22 can be used to feed a parabolic dish increasing its present gain of 6 dB[32] (see Appendix D) to approximately 32 dB.

If the conductivity is increased above .1 mhos/meter monocycle pulses of the order of microseconds must be used. For this case, TEM horns and parabolic dishes become impractical. It has been shown[33] that a Gaussian pulse on a straight wire antenna radiates at the discontinuities. That is, it radiates at the input to the antenna and then again at the end of the antenna. To efficiently radiate a monocycle pulse the conductor should be long enough to support the length of the pulse when it is radiated at the input. The pulse that is radiated at the end of the antenna is usually not wanted and is absorbed by resistors or other dissipative material. To efficiently radiate a .1 μs pulse the antenna, if it is airborne, would be 30.5 m (100 ft) long. However, as discussed in Section 3.6, if the antenna is placed on the water it can be reduced in size by a factor somewhere between 9 and 50 depending on the conductivity of the water. If it is essential that the antenna remain airborne, the antenna can be reduced at the expense of antenna efficiency. Using a slow wave antenna such as a spiral is another

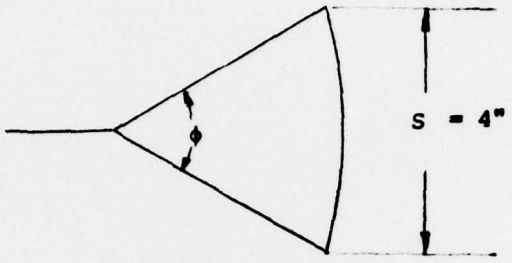

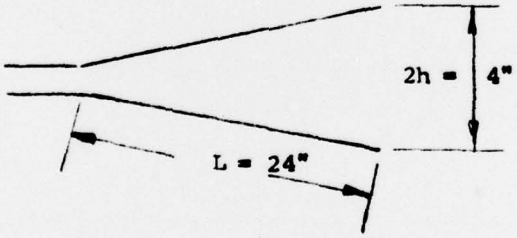

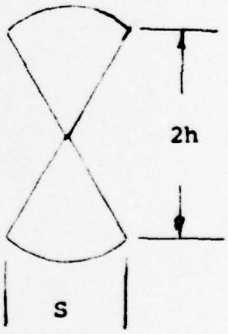

Figure 22. A TEM monocycle antenna that radiates a .5 ns pulse.[31]

alternative for reducing the size.

The techniques used to design single frequency broadband antennas do not always apply to designing antennas to radiate monocycle pulses. For example, "... the concept of optimizing gain-aperture product and {showing} that this criterion is of value for antennas designed to operate over a large bandwidth, ... does not generally lead to antennas capable of radiating picosecond pulses on an instantaneous basis".[34]

5.3 Xmit/RCV Network

The transmit/receive network consists of a device that protects the FET preamplifier in the receive network. There are many forms of the transmit/receive (T/R) section. They must be fast enough and sensitive enough so that they do not degrade the receive signal or the performances of the FET. For the ranges here, recovery time must be extremely short following termination of the transmit pulse.

If high power is transmitted the breakdown rating of the T/R section may be exceeded. For this case separate transmit and receive antennas are used. The receiver can then be protected by sufficiently separating the antennas or by gating the receive channel off when the transmit pulse is radiated.

5.4 FET Preamplifier and Bandpass Filter

The FET preamplifier is the receiver's front end. It must be a low noise

device with sufficient gain to overcome the noise produced by the succeeding portions of the receiver. FET's have a high input impedance and can be found with noise figures of 1 dB, and greatly simplify the design of excellent, broadband receivers of the type required in this application.

A bandpass filter follows the FET preamp to reduce noise and increase the sensitivity of the receive channel. The narrower the bandwidth the greater the sensitivity. The bandwidth of commercial sampling oscilloscopes can be as large as 12 GHz. The antenna size limits the lowest spectral component of the monocycle pulse. The conductivity of the fresh water limits the highest spectral component of the monocycle pulse.

At this time the inverse Fourier transform of the monocycle pulse reflected from the salt water wedge and sandy bottom has not been calculated. The frequency content of the reflected monocycles is not known. It is not possible to accurately chose the center frequency and bandwidth of the transmitted monocycle or the bandpass filter. If it is assumed that the fresh water layer has a low conductivity of .02 mhos/meter, then a monocycle pulse whose width is 10 ns may be used. One over this pulse width yields the highest frequency component of the pulse as 100 MHz. The bandwidth is the 0-100 MHz, but it is impossible to radiate 0 Hz and the antenna acts as a high pass filter. A travelling wave antenna as shown is Figure 14b will be approximately 3 meters long. The highest frequency component of the pulse will penetrate 13 meters; the lower frequencies will penetrate further. The minimum depth at which a salt water wedge can be detected using a monocycle radar 15 meters above a fresh water layer whose constitutive parameters are $\epsilon_2 = 80$ and

σ = .02 mhos/meter is 13 meters. If the broadband folded dipole in Figure 20c is used, the airborne antenna will be approximately 6 meters. If a 25% bandwidth is assumed, the bandpass filter will be 25 MHz. The MDS of the radar is assumed to be -120 dBW, $P_t \doteq$ 10 dBW (10 Watts), and the antenna gain, G, equals 0 dB. The dynamic range is 130 dB. Cook [35] states, "No radar appears feasible with a dynamic range (Performance Figure) exceeding some 280 decibels. Present equipment is still far from this limit." The dynamic range of 130 dB used is conservative compared to 280 dB. Above 30 MHz atmospheric noise becomes negligible and the theoretical MDS, KTB, equals 204 dB below one Joule. In a 25 MHz bandwidth the MDS is -130 dBW.

If some ringing of the transmitted pulse is permissible, it is expected that the antenna can be reduced in size. Moffatt [36] uses an 8.5 meter antenna to radiate a 45 ns pulse. The antenna is approximately half a pulsewidth. Morey [37] uses a .3 meter antenna to radiate a 3 ns pulse. The antenna is approximately one third the pulsewidth.

Summarizing the results for the assumptions made above, the bandpass filter will be 75 MHz to 100 MHz with a center frequency of 87.5 MHz. The depth of penetration through a fresh water layer with the constitutive parameters of $\varepsilon_2 = 80$ and $\sigma_2 = .02$ mhos/meter will be a minimum of 13 meters. The antenna, a folded dipole, will be 6 meters but may be reduced to 2 - 3 meters probably at the expense of efficiency. This will be determined by experimentation. The bandwidth of operation is 25%.

If it is assumed that the fresh water has a high conductivity of 1 mho/

meter, the monocycle pulsewidth will be increased to 1 μs. The antenna will have to be placed on the water, as discussed in Section 3.6, to avoid the energy lost due to reflection at the air/water interface and to take advantage of the loading of the water. The length of the antenna in air would have to be 305 meters to support the pulse. A folded dipole will be twice that or 610 meters. The high conductivity will load the antenna by approximately a factor of 50 reducing the length to 12 meters. The results obtained from the computer model of the West Gotland Basin showed that for a conductivity of 1.2 mhos/meter the loading factor on the antenna may be as high as 80. It may be possible to reduce the antenna's size after Moffatt[36] and Morey,[37] to 6 or 4 meters. As stated in Section 3.5, the concept of loading by a factor of 50 or 80 remains to be proven. The efficiency of a folded dipole 4, 6 or 12 meters long radiating a 1 μs pulse must be determined by experimentation. The highest frequency component of the 1 μs pulse is 1 MHz. It will penetrate 5 meters; the lower components will penetrate further. The minimum depth at which a salt water wedge can be detected using a monocycle radar with its antenna on the "fresh" water whose constitutive parameters are $\varepsilon_2 = 80$ and $\sigma = 1$ mhos/meter is 5 meters. If a 25% bandwidth is assumed, the bandpass filter will be .25 MHz. As explained in Section 3.1, the MDS of the radar is assumed to be -90 dBW, $P_t \doteq$ 30dBW (1k Watt) and the antenna gain, G, equals 0dB. If the antenna gain is -10dB, P_t will be increased to 40 dBW (10k Watt). The noise floor of the 10 k Watt transmitter will have to be less than at most equal to -90 dBW.

Summarizing the results for the assumptions made when the conductivity of the fresh water layer is 1 mho/meter, the bandpass filter will be .75 MHz to

1 MHz with a center frequency of .875 MHz. The antenna of the monocycle radar will have to be on the water and the minimum depth of which a salt water wedge can be detected is 5 meters. The minimum depth of 5 meters is obtained from the computer data presented in Figures 14 thru 17.

5.5 Sample and Hold Circuits

The sample and hold (SAH) circuit in the block diagram of the monocycle radar represents a special class of SAH circuits that are commercially available. To obtain the speed necessary to sample each pulse individually the SAH circuits will probably use hot carrier diodes.

5.6 Integrator

After the analog data has been digitized integration is simply an incoherent summation of data values. Schematically the integration is shown in Figure 23.[38] Setting $B_1 = 1$ integrates E_i. If B_1 is made less than unity an exponential decay results similar to the response of an R C integrator. The signal must be processed so that it is not bipolar. This is done at the expense of information contained in the pulse. Such an integrator is applicable only to case where input SNR's are >0 dB. If necessary additional amplification will take place after the A/D converter.

5.7 Microprocessor

The Microprocessor will analyze the return monocycle pulses that are backscattered from boundaries with varying σ, ϵ and/or μ. The analysis will consist of an autocorrelation of the backscattered signal with anticipated

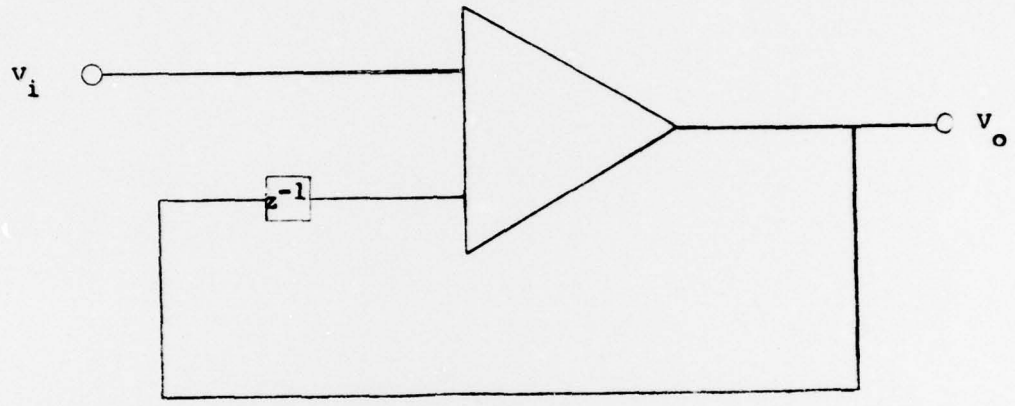

$$V_o = V_i \left(\frac{z}{z - B_1 z} \right)$$

where

z = the variable of the Z transform

B_1 = weighting function

Figure 23. Integrator [38]

monocycle shapes from salt water wedges and different types of estuarian bottoms. The anticipated shapes will be either calculated or measured and stored in peripheral equipment. If the volume of data and or comparisons or autocorrelations that must be made becomes too large a mini-computer will be used.

5.8 Conclusion

A monocycle radar which it is expected can detect and identify salt water wedges in estuaries and be used in bathymetry has been described in a general sense. The transmit section consists of a trigger generator and a monocycle pulse generator that will transmit nanosecond or microsecond pulses, depending on the conductivity of the fresh water layer. Common to both the transmit and receive sections are the T/R network which protects the receiver from the transmitted monocycle pulse and a T/R dipole antenna. The receive section consists of an FET preamplifier, a bandpass filter, SAH circuit and amplifier, an A/D converter, an integrator and a microprocessor.

The bandpass filter follows the FET preamplifier to reduce noise and increase the sensitivity of the receive channel. Advances in switching technology permits picosecond pulses to accurately sample and reproduce a single nanosecond pulse. This permits incoherent envelope integration of a train of monocycle pulses improving system operation at the expense of phase information.

A possible design configuration of a TEM horn feeding a parabolic dish is described that may be useful where 1 nanosecond pulses can penetrate the

water; i.e. when the conductivity is less than .01 mhos/meter.

A specific example of center frequency, bandwidth, pulsewidth, transmitted power and MDS has been given for an airborne monocycle radar 15 meters above a fresh water layer whose conductivity is .02 mhos/meter. Another specific example is given for a monocycle radar whose antenna is on fresh water whose conductivity is 1 mho/meter. The same parameters as specified for the airborne case are given.

It is expected that for the airborne case the antenna will be less than 6 meters and that it will be possible to detect a salt water wedge greater than 13 meters below fresh water whose conductivity is .02 mhos/meter. For the case with the antenna on the water, it is expected that the antenna will be less than 12 meters long and that it will be possible to detect a salt water wedge 5 meters beneath a fresh water layer whose conductivity is 1 mho/meter. It will take experimentation and further computer analysis and design to prove these results.

APPENDIX A

UNITS OF THE CONDUCTIVITY EQUATION

The loss tangent or power factor is defined as the ratio of the conduction current to the displacement current:

$$\tan\delta = \sigma E/\omega\varepsilon E \qquad \text{(A1)}$$

where

σ = the conductivity, mhos/meter

ω = $2\pi f$, angular frequency, radian/sec

f = frequency, Hertz

ε = $\varepsilon_r \varepsilon_o$ Farads/meter

ε_r = the relative dielectric constant of the material

ε_o = 8.854×10^{-12}, Farads/meter

δ = The angle between the conduction current and the displacement current, degrees

From equation (A1) it is seen that

$$\sigma = \omega\varepsilon \tan\delta \qquad \text{(A2)}$$

Subsituting $\varepsilon = \varepsilon_r \varepsilon_o$ and $\omega = 2\pi f$ into equation A2

we have

$$\sigma = 2\pi f \varepsilon_r \varepsilon_o \tan\delta \qquad \text{(A3)}$$

and

$$\sigma = 2\pi f \varepsilon_r 8.854\times10^{-12} \tan\delta$$

$$= 55.63\times10^{-12} f \varepsilon_r \tan\delta$$

$$= f \varepsilon_r \tan\delta \,/\, .0179\times10^{+12}$$

$$= f \varepsilon_r \tan\delta \,/\, 1.79\times10^{-10} \text{ mhos/meter}$$

APPENDIX B

A MONOCYCLE RADAR USED IN OTHER DISSIPATIVE MEDIA

By changing the value of dielectric constant and conductivity in the computer model, the depth of penetration of a monocycle into other materials can be determined. If the material is changed to earth, glacial ice or trees a much larger portion of the energy enters the layer. This is because the relative dielectric constant of these materials is less than that of water. The relative dielectric constant of dry earth is 7. The power reflected from dry earth is

$$P_{ae} = P_t\{(\sqrt{7}-1)/(\sqrt{7}+1)\}^2 = 10kW\{.20\} = 2kW \qquad (B1)$$

where it is assumed the transmitted power, $P_t = 10$ kW.

For the case of dry earth, 80% of the power in the energy in the monocycle pulse enters the earth. If the medium is glacial ice instead of dry earth, 92% of the energy in the monocycle pulse enters. In a manner similar to equation B1 the reflected power is calculated:

$$P_{ai} = P_t\{(\sqrt{3.2}-1)/(\sqrt{3.2}+1)\}^2 = 10kW(.08) = .8kW \qquad (B2)$$

where $\varepsilon_r = 3.2$ and $\sigma = .2\times10^{-6}$ mhos/meter.

If for simplicity one considers trees to represent a smooth homogeneous

interface to a monocycle pulse, the reflected power is

$$P_{at} = P_t\{(\sqrt{2}-1)/(\sqrt{2}+1)\}^2 = 10kW(.03) = 3kW \qquad (B3)$$

where $\varepsilon_r = 2$ and σ and $= 4.4\times10^{-4}$ mhos/meter and 97% of the power enters the trees.

When the conductivity of the materials is considered the characteristic impedance is a complex number defined as

$$\bar{\eta} = \{j\omega\mu/(\sigma+j\omega\varepsilon)\}^{1/2} \qquad (B4)$$

For dry earth it can be shown that

$$\bar{\eta} = 1.42\times10^2 \ \underline{/.735^\circ} \qquad (B5)$$

The angle associates with the impedance is a characteristic of the dissipative medium. It signifies the power in the medium has a real and imaginary part. In general the Poynting vector is therefore not in the same direction as the complex propagation constant.

To determine the ability of a monocycle pulse to detect water under glacial ice, the following model is used. The monocycle radar is assumed 1 meter above 3.7 kilometers (12 ft) of glacial ice. The relative dielectric constant of the glacial ice is 3.2. Its conductivity is 2×10^{-7} mhos/meter. The glacial ice is on a semi-infinite layer of water with the constitutive parameters of $\varepsilon = 80$ and $\sigma = .001$ mhos/meter. Table BI presents the data

TABLE BI

Ratio of received power to transmitted power, P_r/P_t (dB), for various frequencies f(MHz) for 3.7 km of glacial ice over fresh water.

f (MHz)	P_r/P_t (dB)
25	-29.45
50	-35.47
100	-41.49
200	-47.51
300	-51.03
400	-53.53
500	-55.47

where the constitutive parameters are:

a. glacial ice, $\epsilon_r = 3.2$ and $\sigma = 2 \times 10^{-7}$ mhos/meter

b. fresh water, $\epsilon_{fw} = 80$ and $\sigma_{fw} = .001$ mhos/meter

for spectral components of a monocycle pulse. It is assumed that the spectral content of the monocycle pulse is between 25 and 500 MHz. The results shows that it is possible to detect water under 3.7 kilometers of glacial ice.

APPENDIX C

APPROXIMATING THE CHARACTERISTIC IMPEDANCE OF THE FRESH WATER LAYER

In Section 3 the effect of losses in the fresh water layer on the characteristic impedance are neglected. They are accounted for as a loss in energy due to attenuation. It is the purpose of this appendix to show that the assumption is valid for the conductivities and frequencies used. In particular Table III presents oneway attenuation for conductivities ranging from .001 to .1 mhos/meter and frequencies ranging from 25 to 500 MHz.

The basic equation that must be satisfied is

$$\omega\varepsilon >> \sigma \qquad \text{(C1)}$$

This is another way of stating the displacement current is much larger than the conduction current. The worst case occurs when σ = .1 mhos/meter and f = 25 MHz. For these values equation (C1) becomes

$$(2\pi)\ 25\text{x}10^{6}\text{x}\ 8.854\text{x}10^{-12} >> .1$$

and .0014 is not much greater than .1.

Therefore, equation (D1) is not satisfied

The characteristic impedance for the fresh water layer in Section 3 is assumed to be

$$\eta_2 \doteq \sqrt{\mu_o / \varepsilon'_{fw}} \qquad \text{(C2)}$$

where

$$\varepsilon'_{fw} = \varepsilon_{fw} \varepsilon_o \text{ Farad/meter} \qquad \text{(C3)}$$

Substituting equation (C3) into (C2) we have

$$\eta_2 \doteq \sqrt{\mu_o \varepsilon_{fw} \varepsilon_o} \qquad \text{(C4)}$$

Let

$$\varepsilon_{fw} = 80$$
$$\varepsilon_o = 8.854 \times 10^{-12} \text{ Farad/meter}$$
$$\mu_o = 4\pi \times 10^{-7} \text{ Henry/meter}$$

So that

$$\eta_2 \doteq \sqrt{4\pi \times 10^{-7} / 80 \times 8.854 \times 10^{-12}} = 42.12 \text{ Ohms} \qquad \text{(C5)}$$

Recalculating η_2 without making any approximations results in the following value for η_2:

$$\bar{\eta}_2 = \{ j\omega\mu_o / (\sigma_{fw} + j\omega\varepsilon_{fw}) \}^{1/2} \qquad \text{(C6)}$$

where

$\omega = 2\pi f = 2 \times 25$ MHz

$\mu_o = 4\pi \times 10^{-7}$ Henry/meter

$\sigma_{fw} = .1$ mhos/meter

$\varepsilon_{fw} = 80 \times 8.54 \times 10^{-}$ Farad/meter

So that

$$\bar{\eta}_2 = (1.322 \times 10^3 \angle 42.3)^{1/2} = 36.36 \angle 21.15° \text{ Ohms} \quad \text{(C7)}$$

The difference between the magnitude of $\bar{\eta}_2 = 36.36$ Ohms and $\eta_2 = 42.12$ Ohms is 5.76 Ohms. The error, not including power lost due to the imaginary component, is approximately 16%, roughly 8 dB.

When .01 mhos/meter is used to determine what the error in the next to the last column of Table III is we find:

$$\bar{\eta}_2 = 42.3 \angle 2.6° \quad \text{(C8)}$$

and the error is negligible.

APPENDIX D

INCREASE IN ANTENNA GAIN BY FEEDING A PARABOLIC DISH WITH A TEM ANTENNA

The TEM antenna [40] shown in Figure 16 can be used to feed a parabolic dish increasing its present gain from 6 dB [41] to approximately 25 dB. The approach is not meant to be rigorous but rather give the reader a qualitative idea of how the gain of an antenna that radiates a .5 ns pulse (approximately) can be increased. The dimensions of the antenna in Figure 16 is 4 inches x 4 inches. Its gain is calculated to be 6 dB [42] using the following single frequency formula:

$$G = 27000/\phi\theta \qquad \text{(D1)}$$

where

θ = 40° at the 3 dB point

and ϕ = 180° approximately

The assumption that ϕ = 180° is made because the TEM antenna described[40] has no side walls (See Figure 16). The factor 27,000 assumes an efficiency of approximating 65%. Substituting the values for θ and ϕ into D1 yields

$$G = 27{,}000/40\text{x}180 = 3.75 \doteq 6 \text{ dB} \qquad \text{(D2)}$$

The effective wavelength that results in this gain for an aperture of 16 inches squared is

$$G = 4\pi A/\lambda^2 = 4\pi x16/\lambda^2 = 3.75 \qquad (D3)$$

and

$\lambda = .18$ meters

or $f = 1.6x10^9$ Hz

For a parabolic dish with a circular aperture whose diameter is 3 meters and assuming a 70% illumination efficiency,

$$G \doteq .7\times 4\pi A/\lambda^2 = .7x4\pi x7/(.18)^2 = 32 \text{ dB} \qquad (D4)$$

This result is not rigorous and is only presented to show that it may be possible to substantially increase the directivity of snort pulse monocycle antennas by using methods similar to those used for single frequency antennas. The concept remains to be proven.

REFERENCES

(1) Coleman, James; Personal communication at contractor conference, Louisiana State University, Baton Rouge, Louisiana.

(2) Ibid.

(3) Cook, J.C.; "Proposed Monocycle-Pulse-Very-High-Frequency Radar for Airborne Ice and Snow Measurement", Communications and Electronics, AIEE, November 1960 pg 591.

(4) Daley, John; An Empirical Sea Clutter Model, NRL, Oct 1973 AD-769-666 pg 30, 31.

(5) Barrick, Donald E.; "Wind Dependance of Quasi-Specular Microwave Sea Scatter", IEEE Transaction on Antennas and Propagation January 1974 pg 135.

(6) Skolnik, Merrill I.; A Review of Radar Sea Echo, NRL Memorandum Report 2025 July 1969 (AD-693452) pg 12.

(7) Ibid. pg 15

(8) Op. Cit. Daley, John, pg 4

(9) Skolnik, Merrill I,; Introduction to Radar Systems, McGraw Hill, 1962; pg 4.

(10) Op. Cit. Daley, pg 3

(11) Barrick, Donald E.; "Rough Surface Scattering Based on the Specular Point Theory", IEEE Transaction on Antennas and Propagation Vol. AP-16, No. 4, July 1968, pg 452.

(12) Daley, J.C.; Ransone Jr.; J.T.; Davis, W.T.; Radar Sea Return Joss II, NRL Report 7534, pg 8-9.

(13) Adler, Richard B; Chu, Lan Jen; Fano, Robert M.; Electromagnetic Energy Transmission and Radiation, John Wiley & Sons, Inc, New York, 1963 pg 428.

(14) CCIR, World Distribution and Characteristics of Atmospheric Radio Noise, Documents of the Xth Plenary Assembly, Geneva, 1963, Report 322, pg 22.

(15) Von Hippel, Arthur R., ed.; Dielectric Materials and Applications, The MIT Press, Ma. 1954 pg 361.

(16) Herdendorf, Charles E.; Lake Erie Physical Limnology Cruise, Midsummer 1967, Report of Investigation #79, pg 9.

(17) Von Hippel, Arthur R.; ed Dielectric Materials and Applications, The MIT Press, Mass 1954 pg 294.

(18) Ibid.

(19) Ibid pg 361

(20) Downing,George; Waterways Experiment Station, Vicksburg Mississippi; 38180 Private Communication

(21) Magaard, L; Rheinheimer, G; Meereshunde der Ostsee, Springer-Verlag, Berlin, 1974, pg 45.

(22) King, Ronald W.P.; "The Many Faces of the Insulated Antenna", Proceedings of IEEE, Vol. 64, No. 2, February 1976, pg 233.

(23) Skolnik, Merrill I., Introduction to Radar Systems, McGraw Hill 1962, pg 527-528.

(24) Op. Cit. King pg 233.

(25) Op. Cit. Adler, Richard B, pg 405.

(26) Kraichman, Martin B.; Handbook of Electromagnetic Propagation in Conducting Media, Superintendent of Documents, U.S. Government Printing Office, Washington, D.C. 20402, pg 2-2

(27) Brigham, Oran E.; The Fast Fourier Transform, Prentice Hall, N.J.; pg 85.

(28) Ibid. pg 83.

(29) King, Ronald W.P.; Harrison, Charles W., Jr; "The Transmission of Electromagnetic Waves and Pulses Into The Earth", Journal of Applied Physics, Vol. 39, No. 9, 4444-4452, August 1968 Pg 4447.

(30) Kraus, J.D.; Antennas, McGraw Hill, 1950 pg 152.

(31) Susman, Leon; Lamensdorf, David; Picosecond Pulse Antenna Techniques, RADC-TR-70-205 pg 27.

(32) Ibid. pg 46.

(33) Row, R.V.; Morey, R.M.; Bertram, C.L.; Theoretical Analysis of Impulse Propagation in Dissipative Medium, ONR TR. No. 005-73, May 1973, pg 4-9.

(34) Susman, Leon; Lamensdorf, David; Picosecond Pulse Antenna Techniques, RADC-TR-70-205, Oct 1970, pg iii.

(35) Cook, John C.; "Status of Ground Probing Radar and Some Recent Experience", Proceedings of a Specialty Conference held at New England College, Henniker, New Hampshire, August 1974, pg 180.

(36) Mofatt, David L.; "Subsurface Video Pulse Radars", American Society of Civil Engineers, Proceedings of a Specialty Conference held at New England College, Henniker, New Hampshire August 1974 pg 197.

(37) Morey Rexford M,; "Continuous Subsurface Profiling by Impulse Radar', American Society of Civil Engineers, Proceedings of a Specialy Conference held at New England College, Henniker, New Hampshire August 1974 pg 214.

(38) Skolnik, Merrill I.; Radar Handbook, McGraw Hill, 1970.

BIBLIOGRAPHY

Adler, Richard, B,; Chu, Lan Jen; Fano, Robert; Electromagnetic Energy Transmission and Radiation, Wiley 1963.

Alongi, Anthony V.; Short-Pulse and Wide-Bandwidth High Resolution Radars, pg 83-156. Proceeding of the NATO Advanced Study Institute, Goslar/Harz, F.R.G. September 22 October 3, 1975 pg. 83-156.

Barrick, Donald E.; "Wind Dependance of Quasi-Specular Microwave Sea Scatter," IEEE Transactions on Antennas and Propagation, January 1974.

Barrick, Donald E.; "Rough Surface Scattering Based on Specular Point Theory," IEEE Transactions on Antennas and Propagation Vol. AP-16, No. 4,July 1968.

Beckmann, Petr; Spizzichino, Andre; The Scattering of Electromagnetic Waves from Rough Surfaces, Pergamon Press 1968.

Bechtel, Marley E.; Short Pulse Target Characteristics, Proceeding of the NATO Advanced Study Institute, Goslar/Harz, F.R.G. September 22 October 3, 1975

Bertram, C.L.; Morey, R.M.; Sandler, S.S.; "Feasibility Study for Rapid Evaluation of Airfield Pavements," Air Force Weapons Laboratory Report AFWL-TR-71-178, June 1974.

Bertram, C.L.; Campbell, K.J.; Sandler, S.S.;"Locating Large Masses of Ground Ice with an Impulse Radar System," Proc. of the 8th Int. Symposium on Remote Sensing, (Willow Run Lab. University of Michigan Ann Harbor), Pg 241-260, October 1972.

Biggs, Albert W.; "Dipole Antenna Radiation Fields in Stratified Antartic Media", IEEE Transactions AP-16 No. 4 July 1968 pg 445-448.

Brekhovskikh, Lenoid M,; Waves In Layered Media, Academic Press, 1960.

Brigham, Oran E.; The Fast Fourier Transform, Prentice-Hall, Englewood Cliffs, N.Y., 1974.

Budden, K.G.; Radio Waves in the Ionosphere Cambridge, 1966.

CCIR, World Distribution and Characteristics of Atmospheric Radio Noise, Documents of the xth Plenary Assembly, Geneva, 1963, Report 322.

Coleman, James; Personal communication at customer conference, Louisiana State University, Baton Rouge, Louisiana.

Cook, John C.; "Status of Ground Probing Radar and Some Recent Experience", Proceedings of a Specialty Conference held at New England College, Henniker, New Hampshire, August 1974, pg 175-194.

Cook, John C.; "Proposed Monocycle-Pulse-Very-High-Frequency-Radar for Airborne Ice and Snow Measurement", Communications and Electronics, AIEE November 1960.

Cooley, J.W.; Lewis, P.A.; Welsh, P.D.; "The Fast Fourier Transform and its Applications to Time Series Analysis", Ch. 14 in Kurt Enslein, Anthony Ralston, and Herbert S. Wilf (Eds.), Statistical Methods for Digital Computers, John Wiley&Sons, N.Y., 1977.

Daley, John; An Empirical Sea Clutter Model, NRL AD-769666 October 1973.

Daley, J.C.; Ransone Jr,; J.T.; Davis, W.T.; Radar Sea Return Joss II, NRL Report 7534.

Downing, George; Waterways Experiment Station, Vicksburg, Mississippi; 38180 Private Communication

Felson, Leopold B.; Marcuvitz, Nathan; Radiation and Scattering of Waves, Prentice-Hall, Englewood, N.J., 1973.

Herdendorf, Charles E.; Lake Erie Physical, Limnology Cruise Midsummer 1967, Report of Investigations #79.

Jasik, Henry; ed; Antenna Engineering Handbook, McGraw Hill 1961.

Johnson, Curtis C.; Field and Wave Electrodynamics, McGraw Hill 1965.

Keller, George V.; Frischknecht, Frank C.; Electrical Methods in Geophysical Prospecting, Pergamon Press, 1970.

Kennaugh, E.M.; Moffatt, D.L.; "Transients and Impulse Response Approximations", Proceedings of the IEEE, August 1965, pq 893-901.

Kerr, Donald E.; Propagation of Short Radio Waves, McGraw Hill, 1951

King, Ronald W.P.; "The Many Faces of the Insulated Antenna", Proceedings of the IEEE, Vol. 64, No. 2, February 1976 .

King, Ronald W.P.; Harrison, Charles W., Jr; "The Transmission of Electromagnetic Waves and Pulses Into the Earth", Journal of Applied Physics, Vol. 39, No. 9, 4444-4452, August 1968 .

Kong, Jin Au; Theory of Electromagnetic Waves, John Wiley & Sons, N.Y. 1965.

Kraichman, Martin B.; Handbook of Electromagnetic Propagation in Conducting Media, U.S. Government Printing Office, 1976.

Kraus, J.D.; Antennas, McGraw Hill, 1950 .

Magaard, L; Rheinheimer, G; Meereshunde der Ostsee, Springer-Verlag, Berlin. 1974 .

Mofatt, David L.; "Subsurface Video Pulse Radars", American Society of Civil Engineers, Proceedings of a Specialty Conference held at New England College, Henniker, New Hampshire August 1974 pg 195-212.

Mofatt, David L.; Puskar, R.J.; "A Subsurface Electromagnetic Pulse Radar", Geophysics Vol. 41, No. 3 (June 1976) pg 506-518.

Morey Rexford M,; "Continuous Subsurface Profiling by Impulse Radar", American Society of Civil Engineers, Proceedings of a Specialty Conference held at New England College, Henniker, New Hampshire August 1974 pg 213-232.

Parzen, Emanuel; Modern Probability Theory and Its Applications, Wiley 1964.

Row, R.V.; Morey, R.M.; Bertram, C.L.; Theoretical Analysis of Impulse Propagation in Dissipative Medium, Office of Naval Research, TR No. 005-73.

Simpson, Richard A.; "Electromagnetic Reflection and Transmission at Interfaces Involving Graded Dielectrics with Applications to Planetary Radar Astronomy". IEEE Transactions Vol. Ap-24 No. 1, Jan 1976 pg 17-24.

Sivaprasad, K.; Stotz, K.C.; Susungi, N for N.; "Reflection of Pulses at Oblique Incidence from Stratified Dispersive Media," IEEE Trans. Ant. and Prop., January 1976. pg 95-99.

Sivaprasad K,; Stotz, K.C.;"Reflection of Electromagnetic Pulses from Multilayered Media", IEEE Trans. Geosci. Electron., Vol. GE-11, pg 161-164, July 1973.

Skolnik, Merrill I.; Introduction to Radar Systems, McGraw HILL 1962.

Skolnik, Merrill I.; Radar Handbook, McGraw Hill 1970

Skolnik, Merrill I.; A Review of Radar Sea Echo. NRL Report 2025, July 1969.

Sledge, O.D.; George, S.F.; A Study of Sea Return at Normal and Near Normal Incidence, NRL Report 7005.

Steinbach, Karl; On the Polarization Transforming Power of Radar Targets, Proceeding of the NATO Advanced Study Institute, Goslar/Harz, F.R.G. September 22 October 3, 1975 pg 65-82.

Stiefvater, K.; Van Etten, P.; DiTano, B.; Preliminary Results of the Transient Response of Broadband Antennas, RADC-TDR-70.

Stratton, Julius; Electromagnetic Theory, McGraw Hill, N.Y., 1941

Susman, Leon; Lamensdorf David; Picosecond Pulse Antenna Techniques, RADC-TDR-70.

Tsang, L; Kong, J.A.;"Electromagnetic Fields Due to a Horizontal Electric Dipole Antenna Laid on the Surface of a Two-Layer Medium", IEEE Transactions on Antennas and Propagation, September 1974, pg 709-711.

Tyras, George; Radiation and Propagation of Electromagnetic Waves, Academic Press, 1969.

Von Hippel, Arthur R., ed.; Dielectric Materials and Applications, The MIT Press, MA. 1954.

Wait, James R., ed.; Electromagnetic Probing in Geophysics, The Golem Press, 1971.

Wait, James R.;"Electromagnetic Fields of a Pulsed Dipole in Dissipative and Dispersive Media", Radio Science, Vol. 5 No. 4, pg 733-735. April 1970.

Wait, James R.; Spies, Kenneth R.; "Transient Fields for an Electric Dipole in a Dissipative Medium", Canadian Journal of Physics, Vol. 48, 1970 pg 1858-1862.

Wright, John W.; "Backscattering from Capillary Waves with Application to Sea Clutter", IEEE Transactions April Vol. 14 No. 6, November 1966, pg 749 - 754.

Wright, John W.; "A New Model for Sea/Clutter", IEEE Transactions Vol. April 16, No. 2 March 1968 pg 217-223.